The Hubbard Model for Universal Quantum Computation

Ji, Jiawei

UNIVERSITY OF CALGARY

The Hubbard Model for Universal Quantum Computation

by

Jiawei Ji

A THESIS

SUBMITTED TO THE FACULTY OF GRADUATE STUDIES

IN PARTIAL FULFILLMENT OF THE REQUIREMENTS FOR THE

DEGREE OF MASTER OF SCIENCE

DEPARTMENT OF PHYSICS AND ASTRONOMY

CALGARY, ALBERTA

JANUARY, 2019

Abstract

Quantum circuits based only on matchgates are able to perform nontrivial (but not universal) quantum algorithms. Because matchgates can be mapped to non-interacting fermions, these circuits can be efficiently simulated on a classical computer. One can perform universal quantum computation by adding any nonmatchgate parity-preserving gate, implying that interacting fermions are natural candidates for universal quantum computation. Most work to date has focused on Majorana fermions, which are difficult to realize and manipulate in the laboratory, despite the advantage of topologically protecting quantum information. We instead show that universal quantum computation can be implemented using interacting spinless (spin-polarized) fermions and further propose a scheme for achieving universal quantum computation with the Hubbard model, which may be realized in the laboratory based on current experimental techniques.

Acknowledgements

I would like to take this opportunity to express my gratitude to my supervisor Dr. David Feder, whose significant support and encouragement helped me excel and reach my academic goals during the course of my MSc. I have been very fortunate to conduct research under your guidance and be given a chance to attend the March Meeting, which greatly helps me grow as a tender-foot theorist. Thank you.

I am also indebted to my supervisory committee members, Dr. Barry Sanders and Dr. Peter Høyer. I am sincerely grateful to you all for your invaluable guidances, priceless advices, and constructive criticisms during my MSc research.

Regarding those who helped me as colleagues and friends, I am profoundly obliged to your stimulating and interesting discussions over the past few years. Thank you to Akihiko Fujii, Alex Cameron and Sebastian Garcia for all general support in the group. Thanks is also given to Simon Apers for helping me gain the deep understanding of matchgate at the beginning of my research. Having you fellows in the group is my blessing.

Above all, I much appreciate the loving support from my family members who always respect and encourage me to take the path I desire.

Table of Contents

List of Tables

List of Figures and Illustrations

List of Symbols, Abbreviations and Nomenclature

Symbol	Definition
U of C	University of Calgary
UQC	Universal quantum computation
TB	Tight binding
MBQC	Measurement-based quantum computation
AQC	Adiabatic quantum computation
DC	Direct current
n.n.	Nearest neighbor
g	On-site interaction

Chapter 1

Introduction/Overview of Thesis

Proposed by Richard Feynman in 1982 [1], a quantum computer harnessing the power of quantum-mechanical phenomena, such as entanglement and superposition promises to solve certain problems much more quickly than a classical computer that is constructed by capacitors and transistors. For instance, prime number factorization using Shor's algorithm on a quantum computer is proved to be much more efficient than any currently known algorithms executed on a classical computer [2], in the sense that the number of gates required to perform the algorithm scales more efficiently with the size of the input on a quantum computer. This poses a threat to the current widely-used cryptosystem known as RSA. The past few decades have witnessed the rapid theoretical and experimental development of quantum computing. Different platforms for implementing a quantum computer have been proposed, such as trapped ions [3], linear optics [4], quantum dots [5] and circuit QED [6]. Each has its own advantages and disadvantages [7].

In this thesis, we explore the idea of building a quantum computer based on a different platform: using interacting fermions. In this Chapter, I will provide a brief overview of the central concepts to be discussed in the thesis to guide readers through how to construct such a quantum computer. Details on all of these topics will be reviewed throughout the thesis.

Matchgates, first proposed by Valiant, are a special class of two-qubit quantum gates that can perform nontrivial quantum algorithms but are not universal [8]. Quantum circuits composed of these quantum gates defined in the context of graph theory can be efficiently simulated on a classical computer. In contrast, the well-known Clifford gates [9, 10], though also classically simulatable in polynomial time, have no overlap with matchagtes. Matchgates can be extended to universal quantum computation (UQC) by adding the SWAP operation

and this is further generalized to any parity-preserving nonmatchgate unitary [11, 12]. A similar argument is also applicable to Clifford gates: quantum universality occurs when any other gate that is not a Clifford gate is added.

It has been shown that matchgates physically correspond to non-interacting fermions in one dimension, meaning that non-interacting fermions are also classically efficiently simulatable [13–15]. Perhaps this is not surprising, because the wave function for non-interacting fermions can be characterized by a determinant which is computable in polynomial time on a classical computer. Additionally, Terhal and Divincenzo demonstrated that the efficient classical simulatability of non-interacting fermions still remains even with adaptive measurements in the computational basis which is encoded in the presence and absence of a fermion in the mode [13]. This result is in a remarkable contrast with the linear optical quantum computing scheme known as the KLM scheme, where non-interacting bosons together with post-selection suffice to achieve universal quantum computation [4]. Fascinatingly, if the previous measurement scheme is modified to the case where qubits are encoded in the spin states while measurements are performed on spatial locations of fermions, non-interacting fermions would be elevated to universal quantum computation [16].

Nevertheless, non-interacting bosons are not classically efficiently simulatable due to the fact that their wavefunction is described by the permanent, which is #P-hard [17]. This is closely tied to the boson sampling problem which is an intermediate model between quantum universality and efficient classical simulatability [18]. It tells us that the sampling of bosonic probability distributions, where bosons are scattered by a linear-optical network, is hard to simulate on a classical computer because the complexity of determining the permanent is #P-hard. However, the situation with interacting bosons compared to the case of fermions is ironically reversed when we try to approximate the ground states. It is possible to efficiently compute the approximate ground state of bosons efficiently on a classical computer using quantum Monte Carlo methods [19]. In contrast, it is shown to be NP-hard to find the

approximate ground state of interacting fermions due to the sign problem [20], where given a desired error, the computing time grows exponentially with the number of fermions in the system.

The fermionic nature of matchgates plus the ability to extend the framework to UQC imply that interacting fermions could be natural candidates for universal quantum computation. In fact, it has been shown that UQC is possible with interacting Majorana fermions [21, 22] where quantum information is topologically protected. Majorana fermions have the advantage of being free from errors, but it is extremely difficult to realize these fermions in the laboratory. So far few experiments have unequivocally observed Majorana fermions, let alone control and manipulate them precisely [23, 24]. That said, there is a large current experimental push toward topological quantum computation with Majorana fermions [25].

Motivated by the issues mentioned above, in this thesis I only study conventional fermions, demonstrating that interacting fermions with just nearest neighbor (n.n.) interactions suffice to implement UQC. However, in the laboratory, realizing and controlling n.n. interactions is not an easy task. Therefore, we further consider spin-1/2 fermions, investigating interactions within a family of Hubbard Hamiltonians, i.e. on-site interactions, to find all the experimentally realizable conditions to allow for UQC and discuss the possibility of adapting current experimental techniques to implement our proposal.

My thesis is organized as follows. In Chapter 2, I will begin this thesis by giving an introduction to universal quantum computation, talking about some basic and important concepts in quantum computation. In Chapter 3, I will review the basics of graph theory, mainly including the perfect matching and the Pfaffian which give rise to the matchgate theory and provide an overview of linking matchgates to universal quantum computation. Next, in Chapter 4, I will talk about the physics underlying non-interacting fermions, showing its close relation to matchgates and then provide some background for the tight binding(TB) approximation and the well-known Hubbard model. Chapter 5 presents the proposals for

universal quantum computation based on interacting fermions, discussing all the practical criteria for constructing such a quantum computer. Finally, Chapter 6 contains discussion about the potential implementation of proposed scheme via current experimental techniques and the outlook of this work.

Chapter 2

Universal quantum computation

In this chapter, I will give a brief introduction to quantum computation, discussing some basic definitions such as quantum bits (qubits), quantum gates, and the quantum circuit model for quantum computing, all of which lay the foundation for the work in this thesis. The introduction is partly based on Ref. [26] to which I refer readers for more detailed discussions.

2.1 Quantum bits

In a classical computer, information is presented by classical bits which can take on either the state 0 or 1. A classical bit can be physically implemented by one of two levels of DC voltage. However, the basic unit representing information on a quantum computer is called the quantum bit (qubit) which is the quantum analogue of the classical bit. It is implemented in a two-level quantum system, which makes a striking difference from the classical implementation, i.e. two levels of DC voltage. According to quantum mechanics, a two-level quantum system allows the general state of a qubit to be a coherent superposition of 0 and 1 so it can be written as

$$\alpha \left|0\right\rangle + \beta \left|1\right\rangle, \tag{2.1}$$

where $\left|0\right\rangle, \left|1\right\rangle$ are the basis state of a qubit and the basis set $\{\left|0\right\rangle, \left|1\right\rangle\}$ is referred to as the computational basis and α and β are probability amplitudes. According to the Born rule, the probability of being on state $\left|0\right\rangle$ is $|\alpha|^2$ and being on $\left|1\right\rangle$ is $|\beta|^2$. In addition, these two probabilities must satisfy the following equation:

$$|\alpha|^2 + |\beta|^2 = 1. \tag{2.2}$$

In fact, both α and β can be complex, which means that the information contained in this general state also includes the relative phase of α and β.

As I mentioned above, α and β actually contain four parameters but are also constrained by the conservation of probability, i.e. Eq. (2.2). This would give us two free parameters so they can be written as:

$$\begin{aligned} \alpha &= \cos\frac{\theta}{2}, \\ \beta &= e^{i\varphi}\sin\frac{\theta}{2}, \end{aligned} \tag{2.3}$$

where θ and φ are real numbers, defining a point on a unit three dimensional sphere called Bloch sphere as shown in Fig. (2.1) (Cf. Figure 1.3 of Reference [26]). A general qubit becomes:

$$\cos\frac{\theta}{2}\left|0\right\rangle + e^{i\varphi}\sin\frac{\theta}{2}\left|1\right\rangle. \tag{2.4}$$

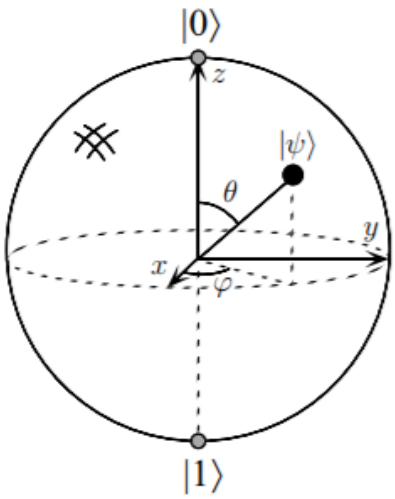

Figure 2.1: The figure shows how a qubit is represented on the Bloch sphere with the probability amplitude $\alpha = \cos\frac{\theta}{2}$ and $\beta = e^{i\varphi}\sin\frac{\theta}{2}$ and the North pole and South pole stand for states $|0\rangle$ and $|1\rangle$ separately.

This is the Bloch representation of a qubit. It is often used to visualize the state of a single qubit. For classical bits, they are either in the North or South pole of this sphere, whereas qubits are able to cover any point on this sphere.

2.1.1 Multiple qubits

Classically, if we have two bits, the possible states would be 00, 01, 10 and 11. Likewise, we can define the basis for two qubits to be $|00\rangle, |01\rangle, |10\rangle, |11\rangle$. Similar to the single-qubit case, two qubits can be in the coherent superposition of all these four quantum states with corresponding probability amplitude associated to each basis state. The following is a general two-qubit quantum state:

$$|\psi\rangle = \alpha_1 |00\rangle + \alpha_2 |01\rangle + \alpha_3 |10\rangle + \alpha_4 |11\rangle , \tag{2.5}$$

where all these four coefficients are complex amplitudes. One can imagine that if we have a general n-qubit quantum state, it would have 2^n computational basis states, taking the form like:

$$|\psi\rangle = \sum_{x_1 x_2 \cdots x_n} \alpha_{x_1 x_2 \cdots x_n} |x_1 x_2 \cdots x_n\rangle, \tag{2.6}$$

where x_k can take on either 0 or 1. Indeed this could be gigantic even if n is just several hundred, so storing such a quantum state on a classical computer is out of the question.

2.2 The quantum circuit model

In the classical computation, we have plenty of classical gates among which the NOR or NAND gates are universal. This means any Boolean function can be implemented merely by either of these two types of logic gates. Analogous to classical circuits, quantum circuits should also be composed of quantum gates to be able to execute arbitrary algorithms. In this section, I will introduce some elementary one and two-qubit gates and discuss the universality of them.

2.2.1 Single-qubit gates

The number of classically nontrivial single bit gates is highly restricted to just one type. It is the NOT gate which maps bit 0 to 1 and 1 to 0, basically flipping bits. Its quantum

analogy-quantum NOT gates must also be capable of mapping a general single qubit state $\alpha|0\rangle + \beta|1\rangle$ to $\alpha|1\rangle + \beta|0\rangle$. In order to find this gate, let us first write this quantum state as a vector:

$$\begin{bmatrix} \alpha \\ \beta \end{bmatrix}. \tag{2.7}$$

The quantum NOT gate shall perform the following operation on this quantum state:

$$X \begin{bmatrix} \alpha \\ \beta \end{bmatrix} = \begin{bmatrix} \beta \\ \alpha \end{bmatrix}. \tag{2.8}$$

It is easy to solve this equation to obtain this matrix X

$$X = \begin{pmatrix} 0 & 1 \\ 1 & 0 \end{pmatrix}. \tag{2.9}$$

This matrix is the desired quantum NOT gate. Moreover, it satisfies $XX^\dagger = X^\dagger X = I$, meaning that it is unitary. In fact, all quantum gates are unitary operations. This comes from the fact that the amplitudes of a general single-qubit state is constrained by Eq. (2.2). The X gate is very important because it is actually one of the so-called Pauli matrices:

$$I = \begin{pmatrix} 1 & 0 \\ 0 & 1 \end{pmatrix}, \quad X = \begin{pmatrix} 0 & 1 \\ 1 & 0 \end{pmatrix}, \quad Y = \begin{pmatrix} 0 & -i \\ i & 0 \end{pmatrix}, \quad Z = \begin{pmatrix} 1 & 0 \\ 0 & -1 \end{pmatrix}. \tag{2.10}$$

These Pauli matrices are of great importance and interest because they are not only unitary but also Hermitian. The unitary matrices generated from the exponentiation of Pauli matrices play a significant role in quantum gates. They are called rotation operators, given as follows:

$$\begin{aligned} R_X(\theta) &= e^{-iX\frac{\theta}{2}} = \cos(\frac{\theta}{2})I - i\sin(\frac{\theta}{2})X, \\ R_Y(\theta) &= e^{-iY\frac{\theta}{2}} = \cos(\frac{\theta}{2})I - i\sin(\frac{\theta}{2})Y, \\ R_Z(\theta) &= e^{-iZ\frac{\theta}{2}} = \cos(\frac{\theta}{2})I - i\sin(\frac{\theta}{2})Z. \end{aligned} \tag{2.11}$$

where I is the identity matrix and θ is a real number. It turns out that any 2×2 unitary matrix can be written in terms of just two of these three rotation matrices:

$$U_{\text{sq}} = e^{i\phi} R_X(\theta_1) R_Z(\theta_2) R_X(\theta_3), \tag{2.12}$$

where sq stands for single-qubit, ϕ is just a global phase that has no observable effect and θ_1, θ_2 and θ_3 are real numbers. This unitary U_{sq} is a generic matrix that maps a single-qubit state to any other single-qubit state. In Fig. 2.1, this implies that any point on the Bloch sphere can be reached by applying this unitary operation. That is why it is often referred to as an arbitrary single-qubit rotation. What it does is to rotate a unit vector pointing to the Bloch sphere to point to another point on the sphere.

Let us check a very special case of the rotation operator, $R_Y(\frac{\pi}{2})$. If we work this out, it becomes:

$$R_Y(\frac{\pi}{2}) = \frac{1}{\sqrt{2}} \begin{pmatrix} 1 & 1 \\ 1 & -1 \end{pmatrix}. \tag{2.13}$$

This gate is called the *Hadamard* gate H. It maps the state $|0\rangle$ to $\frac{|0\rangle+|1\rangle}{\sqrt{2}}$ and the state $|1\rangle$ to $\frac{|0\rangle-|1\rangle}{\sqrt{2}}$. The *Hadamard* gate can be simply understood on the Bloch sphere that it rotates the state $|0\rangle$ by $\pi/2$ to the positive $\mathbf{x}$ axis and the state $|1\rangle$ by $\pi/2$ to the negative $\mathbf{x}$ axis.

2.2.2 Two-qubit gates

Just as in classical computation, where two-bit gates play an important role in computing an arbitrary classical function, such as NOR gate, two-qubit gates are also crucial in executing quantum algorithms, most importantly in forming the universality for quantum computation about which I will talk more later in the section. A two-qubit gate that is vital to many schemes for quantum computation is the CNOT gate. If written in the computational basis, it would be:

$$\text{CNOT} = \begin{pmatrix} 1 & 0 & 0 & 0 \\ 0 & 1 & 0 & 0 \\ 0 & 0 & 0 & 1 \\ 0 & 0 & 1 & 0 \end{pmatrix}. \tag{2.14}$$

It only flips the second qubit when the first one is in the state $|1\rangle$, which is why it is called *controlled* NOT gate conventionally but more precisely speaking, it is the CX gate because the X gate is for qubits while NOT gate is only for bits. Here, the first qubit serves as a controller based on the state of which, the X gate is applied to the second qubit. Let us

apply it to a two-qubit state to see what would happen:

$$\begin{aligned} &\mathrm{CNOT}[(\alpha\,|0\rangle_1 + \beta\,|1\rangle_1) \otimes (\gamma\,|0\rangle_2 + \delta\,|1\rangle_2)] \\ &= \alpha\gamma\,|00\rangle + \alpha\delta\,|01\rangle + \beta\delta\,|10\rangle + \beta\gamma\,|11\rangle\,. \end{aligned} \tag{2.15}$$

One could notice that the resulting two-qubit state can no longer be written as the tensor product of two single-qubit states regardless of the values that α, β, δ and γ could take. Mathematically, it is characterized as follows:

$$|\psi_1\rangle \otimes |\psi_2\rangle \xRightarrow{\mathrm{CNOT}} |\psi'\rangle \neq |\psi_1'\rangle \otimes |\psi_2'\rangle\,. \tag{2.16}$$

This kind of quantum states are referred to as *entangled state* as apposed to the states called *product state* which can be decomposed into the product form of two single-qubit states. The CNOT gate here serves as an entangler to generate the entanglement between two single-qubit states. Once, two qubits are entangled, they no longer can be treated separately but should be regarded as the whole. This is one of many amazing implications of quantum mechanics. Besides, entanglement is responsible for many surprises in quantum computation such as quantum teleportation [27].

There are many other two-qubit gates worth mentioning, one of which is the CZ gate:

$$\mathrm{CZ} = \begin{pmatrix} 1 & 0 & 0 & 0 \\ 0 & 1 & 0 & 0 \\ 0 & 0 & 1 & 0 \\ 0 & 0 & 0 & -1 \end{pmatrix}. \tag{2.17}$$

It only maps state $|11\rangle$ to $-\,|11\rangle$ while leaving other states untouched, conditioned on the state of the first qubit only. The CZ gate is just an special case of the *controlled phase gate* when the phase is set to be π. Different from the CNOT gate, the CZ gate entangles two qubits simply by changing the sign of the state $|11\rangle$ and it can be generated from the CNOT gate and single-qubit gates:

$$\mathrm{CZ} = (I \otimes H)\mathrm{CNOT}(I \otimes H), \tag{2.18}$$

where H is the *Hadamard* gate and I is the *identity* gate. Via the conjugation of H, the CNOT is transformed to the CZ gate.

Finally, I would like to introduce another powerful two-qubit gate, the SWAP gate. In computational basis, it is defined as:

$$\text{SWAP} = \begin{pmatrix} 1 & 0 & 0 & 0 \\ 0 & 0 & 1 & 0 \\ 0 & 1 & 0 & 0 \\ 0 & 0 & 0 & 1 \end{pmatrix}. \tag{2.19}$$

It swaps two qubits. We can easily check this out

$$\begin{aligned} &\text{SWAP}[(\alpha \left|0\right\rangle_1 + \beta \left|1\right\rangle_1) \otimes (\gamma \left|0\right\rangle_2 + \delta \left|1\right\rangle_2)] \\ &= \alpha\gamma \left|00\right\rangle + \alpha\delta \left|10\right\rangle + \beta\delta \left|01\right\rangle + \beta\delta \left|11\right\rangle \\ &= (\gamma \left|0\right\rangle_2 + \delta \left|1\right\rangle_2) \otimes (\alpha \left|0\right\rangle_1 + \beta \left|1\right\rangle_1). \end{aligned} \tag{2.20}$$

This gate is powerful and useful in some cases. However, it can also be produced by applying three CNOT gates consecutively but with one in the middle reversed:

$$\text{SWAP} = \text{CNOT}_{12}\text{CNOT}_{21}\text{CNOT}_{12}, \tag{2.21}$$

where the second CNOT gate is reversed to become the first qubit controlled by the second qubit.

2.2.3 Universal set of gates

In classical computation, it is known that any Boolean function can be computed on a classical computer just using gates from the set $\{\text{NOT}, \text{AND}, \text{OR}\}$ or $\{\text{NAND}\}$ itself, so these sets of gate are universal for classical computation [26]. For quantum computation, a similar principle can be applied to it but is more complicated. If we intend to achieve any arbitrary unitary operation exactly, it would require an infinite set of quantum gates, which is practically impossible. Therefore, one has to approximate the desired unitary operation to arbitrary accuracy ϵ. Let us also give a mathematical definition of ϵ-approximation of a given unitary operation U:

Definition 2.2.1. (Cf. Definition 2.1 of Reference [28]). *An arbitrary unitary operation V, possibly comprising a sequence of quantum gates, provides an ϵ-approximation to a given unitary transformation U if*

$$||U - V|| \doteq \underset{||\psi||=1}{sup} ||(U - V)|\psi\rangle|| < \epsilon, \tag{2.22}$$

The *sup* stands for the supremum norm. It means that when running over all possible normalized input states $|\psi\rangle$, the greatest magnitude would be less than the given error ϵ. Let us give the definition of universal set of gates:

Definition 2.2.2. (Cf. Definition 4.3.1 of Reference [29]). *A set of gates $\mathcal{G}$ is said to be universal if for any integer $n \geq 1$, any n-qubit unitary operator can be approximated to arbitrary accuracy ϵ by a quantum circuit using only gates from that set.*

Quantum universality could be implemented by any two-qubit entangling gate that acts on any pair of qubits when assisted by single-qubit gates [30–33]. There are many choices of universal gate sets, such as {single-qubit gates, CNOT} and {single-qubit gates, CZ } etc. These universal sets can be simplified via replacing single-qubit gates with just two single-qubit rotations, R_X and R_Z, as discussed in Eq. (2.12). Moreover, these two single-qubit rotations could be replaced by set $\{H, S, T\}$ [26], where $T = R_Z(\frac{\pi}{4})$ and $S = R_Z(\frac{\pi}{2})$ up to a global phase, and H is the Hadamard gate. Thus, $\{H, S, T, \text{CNOT}\}$ is a universal set of gates, which is frequently used in experiments. Due to the difficulty in physically implementing a two-qubit entangling gate that acts on any pairs of qubits, the n.n. condition may be imposed, thus the SWAP gate is needed to bring qubits that are further away to the n.n., but its absence shall not effect the universality as we could recall from Thm (2.2.1).

Another important question is raised: How many gates from a universal set does one need to approximate a given n-qubit unitary operation? Or in other words, what is the depth of approximating this unitary operation? It is given by the Solovay-Kitaev Theorem:

Theorem 2.2.1. (Cf. Reference [26]). *Given a universal set of gates $\mathcal{G}$, any unitary operation on n qubits can be ϵ-approximated using $\mathcal{O}(n^2 4^n \log^c \frac{n^2 4^n}{\epsilon})$ gates from the set, where* $c = \lim_{\delta \to 0, \delta > 0} (2 + \delta)$.

The detailed proof can be found in Ref [28]. This important theorem tells us that as long as the number of qubits is fixed, the target circuit scales as the polylogarithm of the desired accuracy, giving us an efficient approximation. The exponential scale in the number of qubits can be attributed to the fact that a 'largest' gate from a given universal set could only act on n' qubits whereas the unitary operations that we desire to approximate should act on n qubits, where $n > n'$ for all n. Thus one could imagine that as n grows, the dimension of the space that these gates are supposed to act on increases exponentially, but the gates from a given universal set remain unchanged size-wise.

Additionally, one also needs to consider how quickly are we able to find the ϵ-approximated break down of any n-qubit unitary operation, i.e. the constructability of such an approximating sequence of gates? It turns out that it is also efficient to construct such a sequence of gates to approximate a given n-qubit gate if the total number of qubits n is fixed [28, 32]. The running time for such a construction varies, depending on if any ancilla qubits and what specific universal set of gates are used in the procedure but typically, it scales polylogarithmically with the inverse of error ϵ.

2.3 The quantum circuit model of computation

So far, I have already discussed quantum data registers (qubits), the basic components of constructing a quantum computer, and universal sets of gates. Let us glue these pieces together to see how exactly a quantum computer works based on the circuit model:

1. **State preparation**: An input quantum state $|\psi\rangle$ can be prepared at the beginning:

$$|\psi\rangle = |x_1\rangle \otimes |x_2\rangle \otimes \cdots \otimes |x_n\rangle \,, \tag{2.23}$$

where $x_n \in \{0, 1\}$ are known as the computational basis states.

2. **Performing any unitary operation**: If there are n qubits in total, quantum gates are required to be applied to any subset of them to implement any desired unitary evolution. This can be done by any universal set of gates as was discussed previously.

3. **Measurement of the output state**: Measurements would be performed on the output state in the computational basis.

This description is the quantum generalization of the classical circuit model. In fact, there are other computational models proposed for implementing universal quantum computation. These models include measurement-based quantum computation (MBQC) [34], topological quantum computation [35] and adiabatic quantum computation (AQC) [36], all of which are essentially equivalent to the quantum circuit model. Moreover, this thesis is primarily concerned with building a quantum computer by constructing quantum gates for UQC.

Chapter 3

Matchgates-based universal quantum computation

In this chapter, I start with reviewing some basic definitions in graph theory, such as perfect matchings and Pfaffians. The discussion is partly based on Valiant's paper [8], which introduces matchgates, and talks about the properties that matchgates possess, particularly the efficient classical simulatability. Finally, I will move on to matchgate-based universal quantum computation, discussing how this special class of quantum gates can be elevated to UQC.

3.1 Perfect matchings and Pfaffians

Before introducing perfect matchings and some other relevant concepts, let me first give a mathematical definition of a weighted and undirected graph: A weighted and undirected graph G is a triple $G(V, E, W)$, where V is a set of vertices, E is a set of edges and W is a set of weights, each weight $w(i, j)$ corresponding to the edge $(i, j) \in E$. The perfect matching is defined as follows. In a connected graph G, with an even number $2k$ of vertices, a matching is perfect if it contains k edges and these k edges share no vertices. Below is an illustration of the perfect matchings:

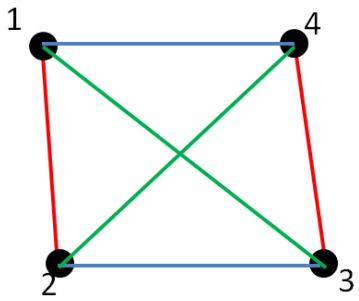

Figure 3.1: The illustration of the perfect matchings in a connected graph. In total, there are three perfect matchings in the graph labeled by three different colors.

Another important mathematical concept is called the Pfaffian, which is based on the perfect matchings. The Pfaffian is a sum of all possible perfect matchings in a graph, with each perfect matching modified by the parity of the number of overlapping pairs. Consider the graph above as an example to explain how the Pfaffian works. There are three different perfect matchings in the graph, $w(1,2)w(3,4)$, $w(1,4)w(2,3)$, and $w(1,3)w(2,4)$. In order to see their connecting relationships more clearly, one may use Chord diagrams:

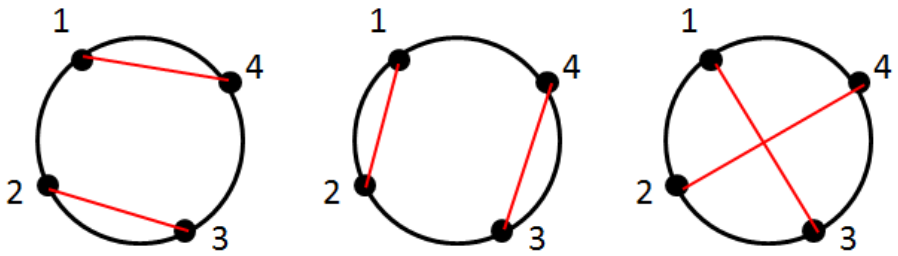

Figure 3.2: This Chord diagram shows the relationships between all the perfect matchings in the graph. Apparently, there no overlaps between first two perfect matchings but there is one overlap in the last perfect matching

This graph's Pfaffian can be written as:

$$\mathrm{Pf}(G) = w(1,4)w(2,3) + w(1,2)w(3,4) - w(1,3)w(2,4), \tag{3.1}$$

where the minus sign in front of the last term is rising from one overlap (odd parity) between the perfect matching $w(1,3)w(2,4)$. So far, I illustrated the Pfaffian in the graphical context whereas in fact it has a mathematical root in the determinant. For each graph $G = G(V,E,W)$, where $V = \{1,2,\cdots,n\}$ there is an $n \times n$ skew-symmetric matrix C associated with it, where each entry is defined as:

$$\begin{cases} w(i,j) & \text{if } i < j, \\ -w(i,j) & \text{if } i > j, \text{ and} \\ 0 & \text{otherwise.} \end{cases} \tag{3.2}$$

The skew-symmetric matrix of the graph in Fig 3.1, then takes the following form:

$$C = \begin{pmatrix} 0 & w(1,2) & w(1,3) & w(1,4) \\ -w(1,2) & 0 & w(2,3) & w(2,4) \\ -w(1,3) & -w(2,3) & 0 & w(3,4) \\ -w(1,4) & -w(2,4) & -w(3,4) & 0 \end{pmatrix}. \tag{3.3}$$

The determinant of this matrix is:

$$\det(C) = (w(1,4)w(2,3) + w(1,2)w(3,4) - w(1,3)w(2,4))^2. \tag{3.4}$$

where the terms inside the bracket corresponds to the Pfaffian in Eq. (3.1). These two representations of the Pfaffian, (mathematically and graphically) are equivalent. In addition, the Pfaffian of an $n \times n$ matrix C is zero if n is odd, because matrix C is anti-symmetric, giving the following facts for odd-dimension matrices:

$$\det(C) = \det(C^T) = \det(-C) = (-1)^n \det(C) = -\det(C). \tag{3.5}$$

This conclusion could be easily understood graphically that any graph that has odd number of vertices fails to make perfect matchings. Hence, these two representations are consistent. Since the Pfaffian is the square root of the determinant of the associated skew-symmetric matrix C, i.e. $\mathrm{Pf}(C)^2 = \det(C)$, it can be computed on a classical computer in a polynomial time, $\mathcal{O}(n^{2.373}), n = 2k$.

Underpinned by the Pfaffian, the Pfaffian sum is graphically defined as a sum of the Pfaffians of all possible sizes

$$\mathrm{PfS}(G) = \sum_S \mathrm{Pf}(G - S) \tag{3.6}$$

where $S \subseteq T$, T is a set of omittable nodes in the graph G. Let us again take the graphs in Fig 3.3 as an example to illustrate this. Here, node 2 is omittable, thus giving us the following Pfaffian sum of the graph G:

$$\mathrm{PfS}(G) = \mathrm{Pf}(G) + \mathrm{Pf}(\tilde{G}), \tag{3.7}$$

where $\tilde{G}$ is called the deleted graph, which is generated after taking away the node 2 from the graph G in Fig. 3.3. Obviously, $\mathrm{Pf}(\tilde{G}) = 0$ because it has an odd number of vertices.

Hence, in this case, $\mathrm{PfS}(G) = \mathrm{Pf}(G)$. The Pfaffian sum can further be transformed to the Pfaffian of a different graph so the efficient classical simulatability can be applied to the Pfaffian sum as well [8].

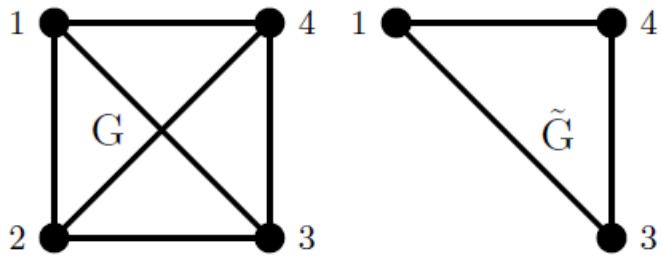

Figure 3.3: The complete graph G has each edge assigned the corresponding weight and a set of omittable nodes is chosen as $T = \{2\}$. The input node is $X = \{1\}$ and output node is $Y = \{4\}$. The deleted graph $\tilde{G}$ is produced after taking away the node 2 from the graph G.

3.2 Matchgates

With these basic graph theory definitions, I shall introduce a special class of gates for simulating quantum gates by what Valiant calls matchgates. A matchgate Γ is a quadruple (G, X, Y, T) where $G(V, E, W)$ is a graph, $X \in V$ is a set of input vertices, $Y \in V$ is a set of output vertices, and $T \in V$ is a set of omittable vertices such that (i) X, Y and T are all disjoint, and (ii) T is between X, Y [8].

$X \cup Y$ are called external nodes. For $Z \subseteq X \cup Y$, the character matrix $\chi(\Gamma, Z)$ of a matchgate is defined as:

$$\chi(\Gamma, Z) = \mu(\Gamma, Z)\mathrm{PfS}(G') \tag{3.8}$$

where: (a) $G' = (V - Z, E', W')$ is the graph where E' is the remaining edges that have both endpoints in $V - Z$, and W' are the corresponding weights of edges E'. (b) $\mu(\Gamma, Z)$ is called modifier, depending on the parity(-1 or +1) of the number of overlaps between E' and external edges. I will take the complete graph G in Fig. 3.3 as a concrete example to illustrate the character matrix. Given omittable vertex $\{2\}$, and input $\{1\}$ and output $\{4\}$, the external nodes Z of this graph G would be $Z = \{1, 4\}$ based on the definition that

$Z \subseteq X \cup Y$, giving rise to four terms to form the character matrix. In this case, the modifier $\mu(\Gamma, Z)$ is always $+1$ because the number of crossings between the external edges that are have an endpoint in external nodes $\{1, 4\}$ and internal matching edges is zero. Hence, we obtain the following entries of the character matrix:

$$
\begin{aligned}
a &= \chi(\Gamma, \emptyset) = w(2,3)w(1,4) - w(1,3)w(2,4) + w(1,2)w(3,4), \\
b &= \chi(\Gamma, \{1\}) = w(3,4), \\
c &= \chi(\Gamma, \{4\}) = w(1,3), \\
d &= \chi(\Gamma, \{1,4\}) = w(2,3).
\end{aligned}
$$

Then the character matrix can be written as:

$$
\chi(\Gamma, Z) = \begin{array}{c} \\ \emptyset \\ 1 \end{array} \begin{array}{c} \begin{array}{cc} \emptyset & 4 \end{array} \\ \begin{pmatrix} a & c \\ b & d \end{pmatrix} \end{array} \tag{3.9}
$$

where the row stands for the input and the column stands for the output. The Eq. (3.9) is called a 1-input, 1-output matchgate with input either $\emptyset$ or in node 1, and output either $\emptyset$ or in node 4. It is simply a gate because a, b, c, d can stand for transition amplitudes from one input state to other output state.

The dimension of the character matrix depends on the number of external nodes. For a graph with 2-input and 2-output nodes, a 4×4 character matrix is obtained. This is what is called a 2-input and 2-output matchgate. From now on, despite the disparity between the character matrix and matchgate, in this thesis I refer to matchgates as character matrices. It is straightforward to generalize to the k-input and k-output matchgate, the character matrix of which is a $2^k \times 2^k$ matrix.

Based on the definition of the character matrix, i.e. Eq. (3.8), it is clear that each entry in the character matrix can be efficiently computed on a classical computer, with the complexity upper bounded by $\mathcal{O}(n^{2.373})$, where n is the number of nodes in the graph used

to construct corresponding character matrix. For a 2-input, 2-output matchgate, a graph with 6 nodes is required to simulate such a matchgate but its character matrix must satisfy Valiant's five matchgate identities [8]. They arise from the Grassmann-Plucker identity that can be traced back to the properties of the Pfaffian [37]. These constraints limit matchgates to take a specific form. Before diving into the details about the specific form that these matchgates could take, I would like to tie matchgates to quantum gates.

For 1-input, 1-output matchagte, this connection is bridged by designating those two possible inputs as $\{\emptyset\} = |0\rangle, \{1\} = |1\rangle$ where $\{\emptyset\}$ and $\{1\}$ represent no input and a input in node 1 respectively[1]. By convention, one would choose rows as outputs and columns as inputs so more precisely, we also need to transpose this character matrix to make it a one-qubit gate. Thus, any single-qubit quantum gate can be achieved by choosing the weights properly to obtain the desired a, b, c, d; even non-unitary gates could be constructed through this character matrix. Therefore, the class of single-qubit matchgates encompasses the class of single-qubit gates.

Regarding the 2-input and 2-output matchgates, one would simply perform the same technique via assigning all four possible inputs as $\{|00\rangle, |01\rangle, |10\rangle, |11\rangle\}$ to transform them to 2-qubit matchgates. Due to the restriction arising from the five identities underpinned by the Grassmann-Plucker identity in the Pfaffian [37], they take the following form:

$$G(A,B) = \begin{pmatrix} A_{11} & 0 & 0 & A_{12} \\ 0 & B_{11} & B_{12} & 0 \\ 0 & B_{21} & B_{22} & 0 \\ A_{21} & 0 & 0 & A_{22} \end{pmatrix} \tag{3.10}$$

where $\det(A) = \det(B)$ and $A, B \in U(2)$. These matchgates are character matrices constructed by corresponding graphs and each entry here in this matrix corresponds to the entry in the character matrix, i.e. Eq. (3.8). Thus, these two-qubit matchgates can be used to simulate certain two-qubit quantum gates and they form a special class of quantum gates

[1] Alternatively, one could consider that $\{\emptyset\}$ and $\{1\}$ represent 'absence' and 'presence,' respectively, to make contact with fermionic field theory, discussed in detail in Chapter4.

that are classically efficiently simulatable. One more thing to notice here is that the even-parity subspace $\{|00\rangle, |11\rangle\}$ and odd-parity subspace $\{|01\rangle, |10\rangle\}$ are completely decoupled.

The quantum states that one could produce using matchgates are not trivial states, that is to say not product states but have entanglement. According to the main theorem in Ref. [8], if two-qubit matchgates that take the form as Eq. (3.10) act on nearest neighbor qubits, any quantum circuit composed of them can be classically efficiently simulated. Immediately a question arises: under what conditions can matchgates be elevated to the universal quantum computation? This will be explored and discussed in the next section.

3.3 Extending matchgates to universal quantum computation

In this section, I would like to talk about how matchgates can combined with other gates to achieve universal quantum computation.

Valiant's main theorem restricts two-qubit matchgates to act only on n.n. qubits. It is reasonable to ask that what would happen if we relax this restriction? In fact, the negative answer was given by the results in Ref. [13] that the quantum circuit consisting of matchgates $G(A, B)$ that could act upon any pair of qubits is still classical efficiently simulatable, which I will discuss in details in next section. Interestingly, Jozsa and Miyake claimed that simply by adding SWAP operations, n.n. matchgate circuits would be elevated to achieve universal quantum computation [11]. I would like to talk about how UQC can be achieved by two-qubit matchgates plus the SWAP gate.

They use a quadrupled number of qubit lines to encode the logical basis states $|0\rangle_L$ and $|1\rangle_L$. The encoding scheme is $|0\rangle_L = |0000\rangle$ and $|1\rangle_L = |1001\rangle$. As shown in Fig. 3.4, in such encoding scheme, the encoded one-qubit gate may be implemented using the following allowed n.n. matchgates:

$$G(Z, X)_{12}G(Z, X)_{34}G(A, A)_{23}G(Z, X)_{12}G(Z, X)_{34}. \tag{3.11}$$

The gate $G(Z, X)$ maps $|0000\rangle$ to $|0000\rangle$ and $|1001\rangle$ to $|0110\rangle$, which moves the quantum

information encoded on line 1 and 4 to 2 and 3. The gate $G(A,A)_{23}$ gate is then applied to lines 2 and 3 to perform arbitrary single-qubit operation A. This single-qubit rotation is achieved due to the fact that the logical qubits after the gate $G(Z,X)$ are in $\{|00\rangle, |11\rangle\}$ subspace of lines 2 and 3. In the end, we move them back via applying the same gates $G(Z,X)$. The left diagram in Fig. 3.4 (Cf. Figure 1 of Reference [11]) is the demonstration of how the encoded single-qubit gate works.

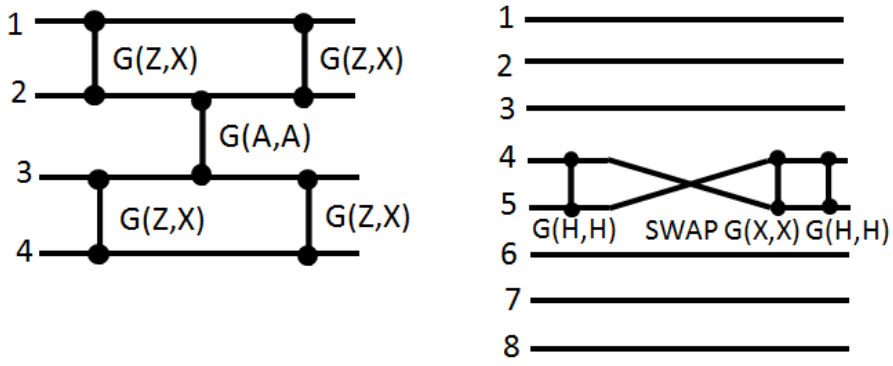

Figure 3.4: The diagrams show how an arbitrary single-qubit gate and n.n. CZ gate are implemented based on the encoding scheme taken here. The n.n. CZ operation is equivalent to applying a sequence of allowed n.n. matchgates and the SWAP gate in the right diagram. Together, they form the universality.

Regarding implementing encoded two-qubit entangling gates, the n.n. CZ gate is chosen to complete the universality of quantum gates. In order to perform universal quantum computation, one needs to entangle any pair of qubits, not just qubits in the nearest neighbor. However, having n.n. CZ gate is sufficient to entangle qubits further away as discussed in Sec. 2.2.3. As shown in the right diagram in Fig. 3.4, to apply the CZ gate to two n.n. logical qubits, one simply applies it to the crossover lines of these two consecutive logical qubits. This is because the general two-logical qubit state encoded on these 8 lines is spanned by

$$|00\rangle_L = |00000000\rangle\,, \quad |01\rangle_L = |00001001\rangle\,, \quad |10\rangle_L = |10010000\rangle\,, \quad |11\rangle_L = |10011001\rangle\,. \tag{3.12}$$

Looking at the crossover lines, i.e. 4 and 5, one could realize that they also form a complete

two-qubit basis. So, the applied CZ gate is

$$\mathrm{CZ}_{45} = \tilde{G}(Z, I) = G(H, H)G(X, X)\tilde{G}(I, X)G(H, H) \tag{3.13}$$

where it is decomposed into some n.n. matchgates and an nonmatchgate gate $\tilde{G}(I, X)$ which is nothing but the SWAP operation. Therefore, universal quantum computation can be performed by n.n. matchgates and the SWAP operations. The SWAP is not matchgate because $\det(I) = -\det(X)$.

However, the conclusion that adding the SWAP gate to n.n. matchgates would perform UQC is paraphrased in their paper as applying a sequence of matchgates that can at most act on the next n.n. qubits [11], that is to say, the relaxation of the nearest neighbor to the next nearest neighbor allows for universal quantum computation. This statement is incorrect because regardless of the SWAP operation, the crossover lines 4, 5 always remain nearest to each other so the role that the SWAP gate plays here is not to swap the quantum information from one wire to another but to break matchgate formalism by being a nonmatchgate gate.

Therefore, one may wonder if is it possible that the gap between n.n. matchgates and universal quantum computation can be bridged by any nonmatchgate gate. It turns out that this is possible if these nonmatchgate also preserve the parity [12]. The nonmatchgate parity-preserving gate takes the same form of any regular matchgate in Eq. (3.10) but is not restricted by the rule of having the same determinants for the odd-parity and the even-parity submatrices. According to Brod and Galvao's results, this kind of gate can take the form:

$$\begin{pmatrix} \cos(a'-b')e^{ic'} & 0 & 0 & i\sin(a'-b')e^{ic} \\ 0 & \cos(a'+b')e^{-ic'} & i\sin(a'+b')e^{-ic'} & 0 \\ 0 & i\sin(a'+b')e^{-ic'} & \cos(a'+b')e^{-ic'} & 0 \\ i\sin(a'-b')e^{ic'} & 0 & 0 & \cos(a'-b')e^{ic'} \end{pmatrix}. \tag{3.14}$$

As long as $c' \neq 0$, it is always a nonmatchgate parity-preserving gate. Obviously, the SWAP gate is in this category, which serves as a hindsight that the previous results could be generalized to any nonmatchgate parity-preserving gate.

Different encoding schemes may be used to implement universal quantum computation.

Distinct from the quadruple encoding where logical qubits are $|0\rangle_L = |0000\rangle$ and $|1\rangle_L = |1001\rangle$, one of the alternatives would be that each logical qubit is encoded in the even-parity subspace of two physical qubits:

$$|0\rangle_L = |00\rangle\,, |1\rangle_L = |11\rangle\,. \tag{3.15}$$

This encoding, employed by Brod and Galvão [12], saves more physical resources than the quadruple encoding where four physical qubits are used to encode each logical qubit. Based on this scheme, the single-qubit rotation is easy to implement. We just need to apply the matchgate $G(A, A)$ to the logical qubits directly. Since the quantum information is encoded in the even-parity subspace, matchgate $G(A, A)$ performs the single-qubit operation in the even-parity subspace. Because a general two-qubit state encoded on these 4 lines is spanned by:

$$|00\rangle_L = |0000\rangle\,, \quad |01\rangle_L = |0011\rangle\,, \quad |10\rangle_L = |1100\rangle\,, \quad |11\rangle_L = |1111\rangle\,, \tag{3.16}$$

the implementation of n.n. CZ gate is achieved by applying it to the crossover lines of two logical qubits, i.e. physical qubits 2 and 3. The CZ gate acting on line 2 and 3 can be written as:

$$\mathrm{CZ}_{23} = G(H, H)G(X, X)\,\mathrm{SWAP}\,G(H, H) \tag{3.17}$$

This is the same as the scheme of implementing the n.n. CZ gate in quadruple encoding, i.e. Eq. (3.13). If one replaces the SWAP gate by the nonmatchgate parity-preserving gate in Eq. (3.14), the implemented entangling gate becomes:

$$\begin{pmatrix} e^{i(a'-b'+c')} & 0 & 0 & 0 \\ 0 & e^{i(a'+b-c')} & 0 & 0 \\ 0 & 0 & -e^{i(-a'-b'-c')} & 0 \\ 0 & 0 & 0 & -e^{i(-a'+b'+c')} \end{pmatrix}. \tag{3.18}$$

It is a nonmatchgate parity-preserving gate because $c' \neq 0$. The actual entangling gates, applied to entangle two logical qubits, are controlled-phase gates. Assisted by single-qubits gates, these two-qubits entangling gates are able to achieve UQC.

Matchgates can be elevated to UQC if any nonmatchgate parity-preserving gate is added, which is similar to the Clifford gates where UQC is achieved when any gate that is not a Clifford gate is added. The long-held conclusion that the relaxation of n.n. matchgates to next n.n. matchgates could perform UQC is wrong, even this is further relaxed to matchgates that could act on any pair of qubits. This is because the matchgate formalism is not dependent on qubit lines. Other than the encoding schemes discussed above, one could adopt another one to perform matchgate-based UQC, which I would talk about in Chapter 5 where the odd-parity subspace encoding is considered to achieve universal quantum computation using interacting fermions.

Chapter 4

Fermions

In this chapter, I will start by giving a brief introduction to second quantization and the well-known tight-binding model. I will then discuss the connections between matchgates and non-interacting fermions in a one-dimensional lattice, showing that matchgates defined in the context of graph theory are physically equivalent to non-interacting fermions. Hence, a quantum circuit based on non-interacting fermions is also efficiently classically simulatable. Finally, the famous Hubbard model is introduced.

4.1 Second quantization

The notations in this section are mostly based on Ref. [38]. In a quantum system consisting of many particles such as bosons or fermions, it is hard to characterize the quantum state of this system using wavefunctions due to the fact that these quantum particles are indistinguishable. The wavefuntions for bosons and fermions are different, the former satisfying the symmetrised property while the latter is antisymmetrised because when two fermions are swapped, there should appear a minus sign. For example, if we have two non-interacting fermions, the wavefunction in the position representation takes the form:

$$\begin{aligned}\Psi(r_1, r_2) =& \frac{1}{\sqrt{2}}(\psi_1(r_1)\psi_2(r_2) - \psi_2(r_1)\psi_1(r_2)) \\ =& \frac{1}{\sqrt{2}} \begin{vmatrix} \psi_1(r_1) & \psi_1(r_2)) \\ \psi_2(r_1) & \psi_2(r_2) \end{vmatrix},\end{aligned} \tag{4.1}$$

where $\psi_i(r_j)$ corresponds to a single-particle wavefunction labeled by quantum number i, for a particle j at position r_j. The determinant is referred to as a *Slater determinant*, used for characterizing the antisymmetry of fermionic wavefunctions. The generalization of the two-particle state above to the N-particle state is quite straightforward, and takes the following

form:

$$\Psi(\cdots, r_i, \cdots, r_j, \cdots) = \frac{1}{\sqrt{N!}} \begin{vmatrix} \psi_1(r_1) & \psi_1(r_2) & \dots & \psi_1(r_N) \\ \psi_2(r_1) & \psi_2(r_2) & \dots & \psi_2(r_N) \\ \vdots & \vdots & \ddots & \vdots \\ \psi_N(r_1) & \psi_N(r_2) & \dots & \psi_N(r_N) \end{vmatrix} \tag{4.2}$$

where the factor $\frac{1}{\sqrt{N!}}$ is the normalization of this quantum state because there are $N!$ ways of permuting N particles, each with equal probability. In contrast, the wavefunction for an N-particle state of bosons is a matrix permanent instead of the determinant, which is the signless version of the determinant. Since determinants are efficient to evaluate on a classical computer whereas permanents are in #P, non-interacting fermions are classically efficiently simulatable but non-interacting bosons are not. It becomes very cumbersome to write the Slater determinant for large N, as the number of terms grows exponentially in N; it is curious therefore that nevertheless the (signed) sum of terms can nevertheless be found efficiently on a classical computer. Instead, the second quantization notation is used to simplify this representation.

In second quantization, particles are treated as excitations of a quantum field; that is to say, instead of writing out all the eigenstates of particles as wavefunctions, one writes the many-particle quantum state in terms of the occupation numbers of particles in different modes. This is known as the occupation number representation and the space spanned by these occupation numbers is called *Fock space*. For example, if one fermion (boson) is in mode k and the other one is in mode l, this many-particle state can be written as:

$$|\Psi\rangle_{k,l} = |0, \cdots, 0, \underbrace{1}_{k}, 0, \cdots, 0, \underbrace{1}_{l}, 0, \cdots, 0, \cdots\rangle \tag{4.3}$$

where 0 represents no particle there and 1 stands for one particle (fermion/boson) in mode k and l. This state is called the Fock basis state and the total vacuum state is the state that has no particle, which is often denoted as $|\varnothing\rangle$.

Another way of looking at the state above is that operators $a_k^\dagger$ and $a_l^\dagger$ have been applied

to create such two particles in these two modes:

$$|\Psi\rangle_{k,l} = a_k^\dagger a_l^\dagger |\varnothing\rangle . \tag{4.4}$$

These are known as creation operators and there are operators that destroy corresponding modes in the state, which is the conjugate of the creation operator known as the annihilation operator. In this case, they are a_k and a_l. In fact, the antisymmetry of fermions is captured by the relations of the fermionic creation and annihilation operators, known as the anti-commutation relations:

$$\{a_k, a_l\} = 0, \quad \{a_k^\dagger, a_l^\dagger\} = 0, \quad \{a_k, a_l^\dagger\} = \delta_{kl}, \tag{4.5}$$

where the bracket $\{\}$ is called the anti-commutator, defined as $\{O, P\} = OP + PO$. In contrast, the symmetry of bosons is captured by the commutation relations of the bosonic creation and annihilation operators:

$$[a_k, a_l] = 0, \quad [a_k^\dagger, a_l^\dagger] = 0, \quad [a_k, a_l^\dagger] = \delta_{kl}, \tag{4.6}$$

where the bracket $[\ ]$ is called the commutator, defined as $[O, P] = OP - PO$. According to the Pauli exclusion principle, at most one fermion could occupy one mode unless more degrees of freedom are introduced such as spin. This directly follows from the second anti-commutation relation in Eq. (4.5):

$$\{a_k^\dagger, a_k^\dagger\} = 2a_k^\dagger a_k^\dagger = 0, \tag{4.7}$$

from which, we immediately obtain $a_k^\dagger a_k^\dagger |\varnothing\rangle = 0$. Whereas for bosons, one mode can be occupied by an arbitrary number of bosons. This can be observed from the commutation relation $[a_k^\dagger, a_l^\dagger] = 0$, which poses no constraint on the number of bosons in each mode.

It becomes convenient to express a general N-particle quantum state in second quantization; for instance, the state in Eq. (4.2) would be compactly written as:

$$|\Psi\rangle = a_1^\dagger a_2^\dagger \cdots a_{N-1}^\dagger a_N^\dagger |\varnothing\rangle \tag{4.8}$$

where $|\varnothing\rangle$ is the total vacuum state. Moreover, observables can also be represented more concisely in second quantization. An n-qubit operator $\hat{\mathcal{O}}$ is typically written as:

$$\hat{\mathcal{O}} = \sum_{i,j=1}^{2^n} \mathcal{O}_{ij} \left|i\right\rangle \left\langle j\right|, \tag{4.9}$$

but in second quantization formalism where the Fock basis is chosen, i.e. where kets and bras are replaced by fermionic creation and annihilation operators, it becomes:

$$\hat{\mathcal{O}} = \sum_{i,j} \mathcal{O}_{ij} a_i^\dagger a_j. \tag{4.10}$$

where $\mathcal{O}_{ij} = \left\langle i\right| \hat{\mathcal{O}} \left|j\right\rangle$. Instead of mapping a basis to another basis, the second quantization formalism allows a particle to be annihilated in a mode and created in another mode. In this sense, both representations are equivalent. Mathematically, one can transform Eq. (4.10) to Eq. (4.9) by sandwiching Eq. (4.10) with two identities:

$$I\hat{\mathcal{O}}I = \sum_k \left|k\right\rangle \left\langle k\right| (\sum_{i,j} \mathcal{O}_{ij} a_i^\dagger a_j) \sum_l \left|l\right\rangle \left\langle l\right|. \tag{4.11}$$

This can be further written as:

$$I\hat{\mathcal{O}}I = \hat{\mathcal{O}} = \sum_{i,j} \sum_{k,l} \mathcal{O}_{ij} \left|k\right\rangle \left\langle k\right| a_i^\dagger a_j \left|l\right\rangle \left\langle l\right|. \tag{4.12}$$

The term $\left\langle k\right| a_i^\dagger a_j \left|l\right\rangle$ survives only when $k = i, l = j$. Hence, Eq. (4.12) is simplified to Eq. (4.9). The second-quantized representation can also be applied to two-particle observables, among which the ubiquitous two-particle interactions are of great importance. In the first-quantized notation, a two-particle observable is written as:

$$\hat{\mathcal{O}'} = \sum_{i,j,k,l=1}^{2^n} \mathcal{O}'_{ijkl} \left|ij\right\rangle \left\langle kl\right|, \tag{4.13}$$

where $\mathcal{O}'_{jikl} = \left\langle ij\right| \hat{\mathcal{O}'} \left|kl\right\rangle$. In the second-quantized representation, it becomes:

$$\mathcal{O}' = \sum_{i,j,k,l} \mathcal{O}'_{ijkl} a_i^\dagger a_j^\dagger a_k a_l. \tag{4.14}$$

I would like to refer readers to Ref. [38, 39] for the rigorous derivations.

4.2 Tight binding model in one dimension

This section covers an important application of second quantization that is widely used in condensed matter physics, known as the tight binding model. The introduction in this section is based on Ref. [40], to which I refer readers for more detailed discussions.

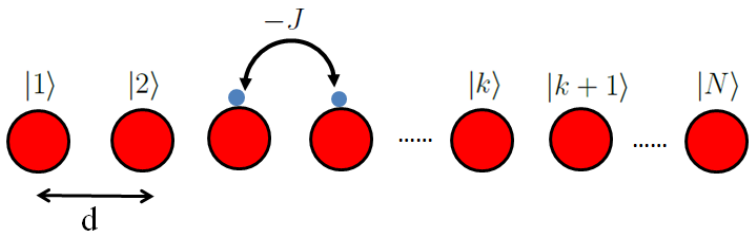

Figure 4.1: The diagram shows a chain of equally spaced atoms in a crystal, each of which is labeled as its own quantum state $|k\rangle$. The electrons can move along this chain but are restricted to the neighboring atoms under the tight-binding approximation with the hopping amplitude $-J$

.

As the picture shown in Fig. 4.1, let us first consider a chain of atoms, each of which has just one atomic orbital at each site in the one-dimensional crystal lattice and the distance d between two neighboring atoms is the same. The electrons would move through the crystal by hopping between nearest-neighboring sites. Each localized atomic orbital is labeled as $|k\rangle, n = 1, 2, \cdots, N$ to represent the basis states, which are equivalent to a set of orthogonal functions localized at different sites, i.e. a site basis. We assume that all these orbitals are orthogonal to one other, i.e.

$$\langle k|l\rangle = \delta_{lk}. \tag{4.15}$$

The general state of the electron can be written as:

$$|\psi\rangle = \sum_l c_l |l\rangle. \tag{4.16}$$

The time-independent Schrödinger equation for this quantum state is:

$$\hat{H}|\psi\rangle = E|\psi\rangle \tag{4.17}$$

and we can simplify it further by inserting Eq. (4.16) and sandwiching it $\langle k|$ from the left:

$$\langle k|\,\hat{H}\sum_l c_l\,|l\rangle = \langle k|\,E\sum_l c_l\,|l\rangle. \tag{4.18}$$

Applying the completeness of the basis states, i.e. Eq. (4.15), it becomes:

$$\sum_l H_{kl}c_l = Ec_k, \tag{4.19}$$

where $H_{kl} = \langle k|\,\hat{H}\,|l\rangle$. Assuming the Hamiltonian only couples nearest neighbor sites while leaving sites that are further away decoupled, one obtains:

$$H_{kl} = \langle k|\,\hat{H}\,|l\rangle = \begin{cases} \epsilon_0 & k = l, \\ -J & k = l \pm 1, \\ 0 & \text{otherwise}, \end{cases} \tag{4.20}$$

where ϵ_0 is the energy of having an electron at a site, often consisting of two parts, $\epsilon_{atom} + V_0$ which are the energies of the atom at that site and a local potential there and $-J$ is the hopping term responsible for the electrons to hop between nearest neighbor sites so sometimes, it is often called the hopping amplitude. Here, the lattice is uniform so ϵ_0 is the same for all sites but generally speaking, it could vary, depending on the lattice site. Therefore, it can be written as ϵ_l.

If we combine these three terms together, we obtain:

$$H_{kl} = \langle k|\,\hat{H}\,|l\rangle = \epsilon_0\delta_{kl} - J(\delta_{k,l+1} + \delta_{k,l-1}). \tag{4.21}$$

Note that the hopping term is $-J$ is negative because it arises from the fact that the hopping is tied to the mean value of the kinetic energy operator $-\frac{\hbar^2}{2m}\nabla^2$ sandwiched by the wavefunctions belonging to the n.n. sites, which is always negative.

If we write this Hamiltonian in the second-quantized representation, it takes the following form:

$$\hat{H}_{\text{TB}} = \epsilon_0\sum_i^N a_i^\dagger a_i - J\sum_{\langle i,j\rangle}(a_i^\dagger a_j + H.c), \tag{4.22}$$

where the local potential ϵ_0 is often written as $-\mu$ and usually is negative. I also refer readers to Ref. [39] for the rigorous derivations of this model in the second-quantized notation.

Though simple, this model can be used to explain many physical phenomena such as crystal band structure and is the foundation of the Hubbard model.

4.3 Wick's theorem

In quantum field theory, Wick's theorem is frequently used to evaluate the expectation value of a string of creation and annihilation operators sandwiched by the vacuum state $|\varnothing\rangle$, by reducing them to the sums of vacuum expectation values of products of pairs of these operators [38, 39]. It can be written as follows:

$$\langle 0|\, A_1 ... A_{2n}\, |0\rangle = \sum (\pm 1)^{\mathrm{p}} \langle A_{i_1} A_{j_1}\rangle ... \langle A_{i_n} A_{j_n}\rangle, \tag{4.23}$$

where the sum runs over all possible permutations of all indices $1...2n$ and p is the number of permutations that take $1...2n$ to $i_1, j_1 ... i_n, j_n$. The sign ± 1 is determined by the types of creation and annihilation operators. If they are fermionic, it takes -1 otherwise it takes $+1$ for bosonic operators. It is clear that unless there are even number of operators in total, this expectation value is always zero, implying that all these operators must be perfectly matched (paired).

Recalling the Paffian discussed in Sec. 3.1, one notices that the Pfaffian actually corresponds to taking quadratic (pairwise) contractions of fermionic expectation values, i.e. Wick's theorem. Here, contractions simply mean calculating the expectation value of each pair of fermionic operators. For instance, the Pfaffian in Eq. (3.1) corresponds to applying Wick's theorem to four fermionic operators:

$$\langle 0|\, A_1 A_2 A_3 A_4\, |0\rangle = \langle A_1 A_2\rangle\langle A_3 A_4\rangle - \langle A_1 A_3\rangle\langle A_2 A_4\rangle + \langle A_1 A_4\rangle\langle A_2 A_3\rangle, \tag{4.24}$$

where A_1, A_2, A_3, A_4 are fermionic operators. In Ref. [13], a similar technique is applied to evaluating the probability that a certain subset of output is obtained with a given input in

a non-interacting fermionic quantum circuit on n fermionic modes. This is shown to be the Pfaffian of a matrix associated with the corresponding subset of output and the given input, which can be computed in poly(n) time classically. Thus, non-interacting fermions are also efficiently simulatable classically. Perhaps this is not surprising, because they are described by Slater determinants as mentioned previously and it is easy to generalize to more particles to be efficiently computed. This is closely related to the efficient classical simulation of fermionic linear optics [13–15].

More important for this thesis, matchgates can be directly constructed through non-interacting fermions. Let us first consider a two-mode fermionic gate. The Hamiltonian can be written as:

$$\hat{H}_{ij} = -\mu_i a_i^\dagger a_i - \mu_j a_j^\dagger a_j - t_{ij} a_i^\dagger a_j - t_{ji} a_j^\dagger a_i, \tag{4.25}$$

where $-t_{ij}$ is the hopping strength corresponding to the fermion hopping from jth site to ith site, and $-\mu_i, -\mu_j$ are the local potential at site i and j. Here, the n.n. restriction is not imposed. This Hamiltonian corresponds to non-interacting fermions hopping between two modes/sites i and j, and an energy offset at a given site. We use inputs $|x_1\rangle = |\varnothing\rangle, |x_2\rangle = a_i^\dagger |\varnothing\rangle, |x_3\rangle = a_j^\dagger |\varnothing\rangle, |x_4\rangle = a_i^\dagger a_j^\dagger |\varnothing\rangle$ as the Fock basis, which form a complete basis so we have the following equation:

$$I = \sum_{k=1}^{4} |x_k\rangle \langle x_k|. \tag{4.26}$$

This allows us to write the Hamiltonian in Eq. (4.25) as:

$$I\hat{H}_{ij}I = \hat{H}_{ij} = \sum_{k,l}^{4} |x_k\rangle \langle x_k| \hat{H}_{ij} |x_l\rangle \langle x_l| . \tag{4.27}$$

Then the term $\langle x_k| \hat{H}_{ij} |x_l\rangle$ corresponds to the matrix element on kth row and lth column so let us calculate them out explicitly. When $k = l = 1$, we have:

$$\langle x_1| \hat{H}_{ij} |x_1\rangle = \langle \varnothing| \hat{H}_{ij} |\varnothing\rangle = 0. \tag{4.28}$$

This is because an annihilation operator acting on the vacuum state gives us zero. Thus, one can imagine that all the elements in the first row and the first column are just zeros

since we always have unbalanced creation and annihilation operators. For instance, when $k = 1, l = 2$, one has:

$$\begin{aligned}\langle x_1|\, \hat{H}_{ij}\, |x_2\rangle = \langle \varnothing|\, \hat{H}_{ij} a_i^\dagger\, |\varnothing\rangle =& -\mu_i \langle \varnothing|\, a_i^\dagger a_i a_i^\dagger\, |\varnothing\rangle - \mu_j \langle \varnothing|\, a_j^\dagger a_j a_i^\dagger\, |\varnothing\rangle \\ & - t_{ij} \langle \varnothing|\, a_i^\dagger a_j a_i^\dagger\, |\varnothing\rangle - t_{ji} \langle \varnothing|\, a_j^\dagger a_i a_i^\dagger\, |\varnothing\rangle \\ =& 0.\end{aligned} \tag{4.29}$$

Every term above is just zero because each contains three creation and annihilation operators, i.e. unbalanced, resulting in zero as they are sandwiched by the vacuum state. However, for $k = l = 2$, one obtains:

$$\begin{aligned}\langle x_2|\, \hat{H}_{ij}\, |x_2\rangle = \langle \varnothing|\, a_i \hat{H}_{ij} a_i^\dagger\, |\varnothing\rangle =& -\mu_i \langle \varnothing|\, a_i a_i^\dagger a_i a_i^\dagger\, |\varnothing\rangle - \mu_j \langle \varnothing|\, a_i a_j^\dagger a_j a_i^\dagger\, |\varnothing\rangle \\ & - t_{ij} \langle \varnothing|\, a_i a_i^\dagger a_j a_i^\dagger\, |\varnothing\rangle - t_{ji} \langle \varnothing|\, a_i a_j^\dagger a_i a_i^\dagger\, |\varnothing\rangle \\ =& -\mu_i.\end{aligned} \tag{4.30}$$

Only the first term survives. The second term contains the annihilation operator a_j that can be pushed through $a_i^\dagger$ to directly act on the vacuum state because they commute according to Eq. (4.5). Thus, it is zero and the same is true for the third term. As for the last term, one could notice that the creation operator $a_i^\dagger$ creates a fermion in mode i first but the annihilation operators a_i annihilates it twice subsequently so still it is zero. Applying the same principle, other matrix elements are found to be:

$$\begin{aligned}&\langle x_2|\, \hat{H}_{ij}\, |x_3\rangle = -t_{ij}, \quad \langle x_3|\, \hat{H}_{ij}\, |x_2\rangle = -t_{ji}, \\ &\langle x_3|\, \hat{H}_{ij}\, |x_3\rangle = -\mu_j, \quad \langle x_4|\, \hat{H}_{ij}\, |x_4\rangle = -\mu_i - \mu_j.\end{aligned} \tag{4.31}$$

The rest of unwritten elements are all zeros as the annihilation and creation operators are also unbalanced in these matrix elements. Therefore, this Hamiltonian becomes the following block-diagonal matrix:

$$H_{ij} = \begin{pmatrix} 0 & 0 & 0 & 0 \\ 0 & -\mu_i & -t_{ij} & 0 \\ 0 & -t_{ji} & -\mu_j & 0 \\ 0 & 0 & 0 & -\mu_i - \mu_j \end{pmatrix}, \tag{4.32}$$

where each block corresponds to a fixed particle number. Now, after taking the exponential of this matrix, we obtain the evolution matrix:

$$e^{-iH_{ij}} = \begin{pmatrix} 1 & 0 & 0 & 0 \\ 0 & b_{22} & b_{23} & 0 \\ 0 & b_{32} & b_{33} & 0 \\ 0 & 0 & 0 & e^{i(\mu_i+\mu_j)} \end{pmatrix} \tag{4.33}$$

where the middle block is the exponential of the corresponding block in the Hamiltonian. In order to show that this gate is a matchgate, we need to prove

$$\det \begin{vmatrix} b_{22} & b_{23} \\ b_{32} & b_{33} \end{vmatrix} = e^{i(\mu_i+\mu_j)}. \tag{4.34}$$

Using Jacobi's identity $\det(e^{sB}) = e^{\mathrm{Tr}(sB)}$ where s is a scalar and B is a matrix, one immediately obtains:

$$\det \begin{vmatrix} b_{22} & b_{23} \\ b_{32} & b_{33} \end{vmatrix} = e^{-i\mathrm{Tr}\begin{pmatrix} -\mu_i & -t_{ij} \\ -t_{ji} & -\mu_j \end{pmatrix}} = e^{i(\mu_i+\mu_j)}. \tag{4.35}$$

Therefore, this gate is a matchgate.

If one adds two more terms to the Hamiltonian above, it would become:

$$\hat{H}'_{ij} = -\mu_i a_i^\dagger a_i - \mu_j a_j^\dagger a_j - t_{ij} a_i^\dagger a_j - t_{ji} a_j^\dagger a_i + \tilde{t}_{ij} a_i a_j + \tilde{t}_{ji}^* a_j^\dagger a_i^\dagger, \tag{4.36}$$

where the two extra terms allow a pair of fermions at site i and j to be created and annihilated with strength $\tilde{t}_{ij} \in Z$. This breaks the conservation of particle number but still preserves the parity. It is similar to the mean-field Hamiltonian for a superconductor [38]. In the same basis as above, this Hamiltonian can be expressed as the matrix:

$$H'_{ij} = \begin{pmatrix} 0 & 0 & 0 & \tilde{t}_{ij} \\ 0 & -\mu_i & -t_{ij} & 0 \\ 0 & -t_{ji} & -\mu_j & 0 \\ \tilde{t}_{ji}^* & 0 & 0 & -\mu_i - \mu_j \end{pmatrix}, \tag{4.37}$$

then taking the exponential of it, we obtain:

$$e^{-iH'_{ij}} = \begin{pmatrix} a_{11} & 0 & 0 & a_{14} \\ 0 & b_{22} & b_{23} & 0 \\ 0 & b_{32} & b_{33} & 0 \\ a_{41} & 0 & 0 & a_{44} \end{pmatrix}, \tag{4.38}$$

where the submatrices **a** and **b** (expressed in terms of the coefficients a_{ij} and b_{ij}, respectively) are the exponentials of the corresponding submatrices in the Hamiltonian because the odd and even-parity subspace are decoupled, resulting in decoupled unitaries. Applying Jacobi's identity to the submatrix **b**, one obtains:

$$\det(\mathbf{b}) = e^{i(\mu_i+\mu_j)}. \tag{4.39}$$

Because the inclusion of off-diagonal elements $\tilde{t_{ij}}$ and $\tilde{t}^*_{ji}$ have no effect on the determinant of the exponential, i.e. submatrix **a**, according to Jacobi's formula. One also obtains:

$$\det(\mathbf{a}) = e^{i(\mu_i+\mu_j)}. \tag{4.40}$$

Therefore, one ends up getting:

$$\det(\mathbf{a}) = \det(\mathbf{b}), \tag{4.41}$$

which demonstrates that this gate is also a matchgate.

Hamiltonians like the one in Eq. (4.36) that involves general quadratic interactions can always be written in a new set of Hermitian operators as:

$$\hat{H'} = \frac{i}{4}\sum_{k,l}\alpha_{kl}c_k c_l, \tag{4.42}$$

where c_k, c_l are known as Majorana fermions, defined as follows:

$$c_{2i} = a_i + a_i^\dagger, \quad c_{2i+1} = -i(a_i - a_i^\dagger). \tag{4.43}$$

One can notice that these operators are Hermitian, i.e. $c_{2i} = c_{2i}^\dagger$ and $c_{2i+1} = c_{2i+1}^\dagger$. Thus, a Majorana fermion is its own antiparticle. Majorana fermions obey the following anticommutation relations:

$$\{c_k, c_l\} = 2\delta_{kl}. \tag{4.44}$$

Applying this anticommutation relation, Eq. (4.42) can rewritten as:

$$\hat{H'} = \frac{i}{4}\sum_{k\neq l}\alpha_{kl}c_k c_l, \tag{4.45}$$

where all terms proportional to identity is ignored. The hermiticity of the Hamiltonian requires that $\mathrm{Im}(\alpha_{kl}) = \mathrm{Im}(\alpha_{lk})$ so typically, the matrix α is chosen to be real and anti-symmetric. Non-interacting Majorana fermions are also shown to be classically efficiently simulatable in Ref. [13] where the Wick's theorem is used again to evaluate the probability of partial sampling of the output. Because the general non-interacting fermionic Hamiltonian can be simply written in the quadratic form, i.e. Eq. (4.45), the unitary arising from this type of Hamiltonian is always a Gaussian operation, which serves as the hindsight that non-interacting fermions is classically poly-time computable [11, 41].

In fact, the encoding schemes discussed in Sec. 3.3 have already implied that the physical carriers are Majorana fermions because the quantum information is encoded in even-parity subspace where the parity is preserved but the conservation of particle numbers breaks. Furthermore, it was originally shown by Bravyi and Kitaev that UQC can be implemented with interacting Majorana fermions [21]. The elevation of non-interacting Majorana fermions to UQC is achieved by four-Majorana particle interactions. Although quantum information is topologically protected using Majorana fermions, it is very challenging to realize these particles in the laboratory, let alone control and manipulate them. Thus, a question is raised: Is it possible to just use conventional interacting fermions to achieve UQC? This question will be answered in next chapter.

4.4 Introduction to the Hubbard model

The tight-binding model is a good approximation for the description of the motion of free electrons in materials that have crystalline structures. However, it fails to consider the interactions between these huge number of electrons moving in the atomic lattice. In reality, the interactions could be short or long-range. Thus, some simplified models based on certain approximations were developed, among which one of the most important is the Hubbard model [39]. It describes spin-1/2 fermions (for example electrons) hopping from one site to

the nearest neighbor sites in the lattice and only interacting with other fermions when occupying the same sites, which is often referred to as on-site interaction. According to Pauli's exclusion principle, two fermions that are able to occupy the same site must have different spins so the on-site interaction is only non-zero when spin-up and spin-down fermions are at the same site.

More specifically, in the second-quantized notation, the Hamiltonian of this model can be written as:

$$\hat{H}_{\text{Hubbard}} = -J \sum_{\langle i,j\rangle,\sigma} (a^{\dagger}_{i,\sigma} a_{j,\sigma} + H.c) + g \sum_{i}^{N} n_{i\uparrow} n_{i\downarrow}, \tag{4.46}$$

where σ indicates the spin projection of the fermion, g is the on-site interaction strength, and $n_{i\sigma} = a^{\dagger}_{i,\sigma} a_{i,\sigma}$ is the number operator for a spin-σ fermion. We should notice that this Hamiltonian would not flip spin and also preserves the particle number in the system. The rigorous derivation of this model can be found in Ref. [39].

The Hubbard model is a good approximation for electrons in a lattice that has a periodic potential when the temperature in the lattice is sufficiently low that all electrons are in the lowest Bloch band and long-range interactions can be neglected as compared to shot range interactions between electrons. Nonetheless, the Hubbard model is only an approximation in a real material due to impurities, phonons, long-range interactions, etc. Optical lattices for ultracold atomic Fermi gases have been proposed as a potentially ideal environment [42] simulating the Hubbard model. Free from impurities, phonons and uncontrollable long-range interactions, an optical lattice is a periodic EM field, formed by the interference of counterpropagating monochromatic laser beams for trapping neutral atoms. By adjusting the well depth and periodicity (by adjusting the laser intensity and geometry), the Hubbard model can be well simulated and studied in optical lattices [43]. In principle, engineering the landscape of the optical lattice could play an important role in achieving the specific goal of quantum simulation and quantum computing with ultracold atoms but an on-going challenge is cooling two-component fermions in optical lattices to very low temperatures [44].

Chapter 5

Universal quantum computation with interacting fermions

In previous chapters, I have reviewed that n.n. matchgates plus any nonmatchgate parity-preserving gate would perform UQC and the physics of non-interacting fermions under the tight-binding model is corresponding to the evolution of n.n. matchgates. Together, this actually implies that interacting fermions could have potential to implement universal quantum computation, analogous to how adding parity-preserving nonmatchgates can lead to UQC, as discussed in Sec. 3.3. In this chapter, I will describe two schemes for introducing interactions between fermions which may achieve universal quantum computation via successfully implementing single-qubit and CZ gates.

5.1 Interacting spin-polarized fermion quantum computer

This section presents how universal quantum computation can be achieved via interacting spinless fermions, by encoding logical qubits in the odd-parity subspace of two physical qubits. The interaction needed here is between nearest neighbors, which may require using dipolar atoms with external electric field to control the interaction strength. Although, this scheme demands extra efforts to be workable, it still offers a potential way forward for achieving UQC.

5.1.1 Single-qubit operations

Recalling the Hamiltonian and unitary for two-mode non-interacting spinless fermions, Eq. (4.32), one can encode logical qubits in the odd-parity subspace:

$$|0\rangle_L = |10\rangle\,, |1\rangle_L = |01\rangle\,. \tag{5.1}$$

Physically this represents the mode a fermions occupies. Nevertheless, these two modes here are nearest neighbors. Conventionally, one would encode as $|0\rangle_L = |01\rangle\,, |1\rangle_L = |10\rangle$, whereas it is more natural if the fermion on the left site is encoded as logical qubit $|0\rangle_L$ and on the right site as $|1\rangle_L$. Previously, the encoding schemes discussed in the Sec. 3.3 adopt the even-parity subspace encoding [11, 12], which requires using Majorana fermions. However, this encoding scheme here only require using conventional fermions because the particle number is also preserved.

Physically, one would have the one-dimensional optical lattice shown in Fig. 5.1 where the red dots represent fermions loaded in the lattice, each only spreading across two sites. This lattice consists of multiple half-filled double-wells, which correspond to the encoding scheme above. These logical qubits are encoded in the spatial modes so there might be an issue that the quantum information encoded here could leak out if these fermions hop to other sites than just stay in the double-well. However, the picture in Fig. 5.1 shows that each double-well is separated from another by a high potential barrier to prevent leakage from one double well to another. If we just look at sites 1 and 2, the Hamiltonian corresponding to it becomes:

$$H_{12} = \begin{pmatrix} -\mu_1 & -t_{12} \\ -t_{21} & -\mu_2 \end{pmatrix} \tag{5.2}$$

where $-t_{12} = -t_{21} = -J_{12} \in \mathbb{R}_{<0}$ stands for the hopping strength between site 1 and 2, which are taken to be positive real numbers, and $-\mu_1, -\mu_2 \in \mathbb{R}_{<0}$ stand for local potentials at sites 1 and 2. This Hamiltonian cane be rewritten as:

$$H_{12} = \begin{pmatrix} -\mu_1 & -J_{12} \\ -J_{12} & -\mu_2 \end{pmatrix} = -J_{12}X + \frac{-\mu_1+\mu_2}{2}Z + \frac{-\mu_1-\mu_2}{2}I, \tag{5.3}$$

where X,Z,I are Pauli matrices. The unitary rising from this Hamiltonian is:

$$U_{12} = e^{-iH_{12}t} = e^{-i(-J_{12}X + \frac{-\mu_1+\mu_2}{2}Z + \frac{-\mu_1-\mu_2}{2}I)t}, \tag{5.4}$$

where t is the evolution time. Recalling from Sec. 2.2.1, we know that an arbitrary single-qubit operation is expressed as:

$$U_{\text{sq}} = e^{-i\frac{\theta_1}{2}X}e^{-i\frac{\theta_2}{2}Z}e^{-i\frac{\theta_3}{2}X}. \tag{5.5}$$

Hence, by tuning the hopping amplitude $-J_{12}$ and evolution time t with two local potentials $-\mu_1$ and $-\mu_2$ turned off, all X-rotation gates could be implemented, and Z-rotation gates can be achieved via tuning two local potentials $-\mu_1$ and $-\mu_2$ and evolution time t with the hopping amplitude $-J_{12}$ turned off. As for the the phase triggered by $-(\mu_1 + \mu_2)$, (the contribution from $\frac{-\mu_1-\mu_2}{2}I$ in Eq. (5.3)), it is simply a global phase, resulting in no practical effect.

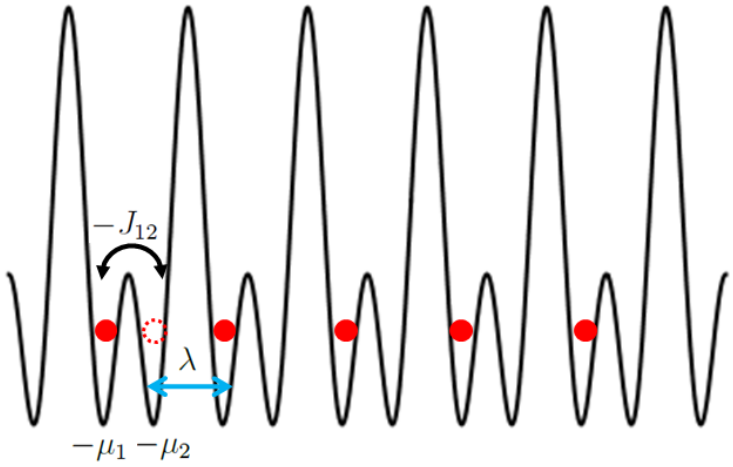

Figure 5.1: This diagram presents that each double-well is loaded with a spin-polarized fermion to encode logical qubits in a one dimensional optical lattice and is separated by a high potential barrier from one and another. The local potentials at sites 1 and 2 are labeled as $-\mu_1, -\mu_2$, and the $-J_{12}$ represents hopping amplitude between site 1 and 2 and the nearest neighbor interaction between site 2 and 3 is λ.

5.1.2 Two-qubit entangling gates

In order to perform UQC, we also need to construct a two-qubit entangling gate as discussed in Sec. 2.2.3. Because our quantum information is encoded in the odd-parity subspace, a general two-qubit quantum state is spanned by:

$$\begin{aligned} |00\rangle_L = |10\rangle_1 \otimes |10\rangle_2 , |01\rangle_L = |10\rangle_1 \otimes |01\rangle_2 , \\ |10\rangle_L = |01\rangle_1 \otimes |10\rangle_2 , |11\rangle_L = |01\rangle_1 \otimes |01\rangle_2 \end{aligned} \tag{5.6}$$

where labelings 1 and 2 stand for logical qubit 1 and 2. Like the scheme employed in Ref. [11], we simply apply a gate on the crossover sites, i.e. on sites 2 and 3 to perform the desired operation on two consecutive logical qubits. Among all two-qubit entangling gates, the CZ gate is chosen to be implemented here. In this encoding scheme, because the logical qubit basis $|11\rangle_L$ is encoded as $|0101\rangle$, applying the CZ gate to logical qubits is equivalent to performing a gate as follows on crossover lines (sites 2 and 3):

$$\tilde{G}(I, Z) = \begin{pmatrix} 1 & 0 & 0 & 0 \\ 0 & 1 & 0 & 0 \\ 0 & 0 & -1 & 0 \\ 0 & 0 & 0 & 1 \end{pmatrix} \tag{5.7}$$

which is a nonmatchgate parity-preserving gate. It cannot be achieved without introducing any interactions beween the fermions. Given that we are (so far) considering spinless fermions, an on-site interaction is not possible due to the Pauli principle. The minimal interaction model therefore corresponds to nearest neighbors:

$$\hat{H}_{\text{tot}} = -\sum_i \left(t_{2i-1,2i} a^\dagger_{2i-1} a_{2i} + H.c\right) - \sum_i \mu_i a^\dagger_i a_i + \lambda \sum_i a^\dagger_{2i} a_{2i} a^\dagger_{2i+1} a_{2i+1}, \tag{5.8}$$

where the hopping amplitude between wells is zero to prevent the leakage of quantum information between double-wells, and the hopping amplitude $t_{2i-1,2i}$ is the hopping amplitude inside wells. λ stands for n.n. interaction strength between wells. This is the Hamiltonian governing 1D lattice plotted in the Fig. 5.1. The first sum stands for the hopping inside double-wells and between wells. The second terms represents the local potentials at each lattice site and the last one is the introduced n.n. interactions between n.n. double-wells.

Based on this Hamiltonian, the two-mode Hamiltonian in the context of sites 2 and 3 becomes:

$$H_{\text{tot}}^{(2)} = \begin{pmatrix} 0 & 0 & 0 & 0 \\ 0 & -\mu_3 & 0 & 0 \\ 0 & 0 & -\mu_2 & 0 \\ 0 & 0 & 0 & -\mu_2 - \mu_3 + \lambda \end{pmatrix} \tag{5.9}$$

Our goal is to implement the $\tilde{G}(I, Z)$ gate so we need to adjust all these parameters. It turns out that the easiest case would be that if we set parameters as following:

$$-\mu_2 = (2m+1)\pi, -\mu_3 = 2n\pi, \lambda = (2l+1)\pi. \tag{5.10}$$

where $m, n, l \in \mathbb{Z}$. Then, after taking the exponential of the matrix above, i.e. $e^{-iH_{\text{tot}}^{(2)}}$, one obtains:

$$e^{-iH_{\text{tot}}^{(2)}} = \begin{pmatrix} 1 & 0 & 0 & 0 \\ 0 & e^{-i2n\pi} & 0 & 0 \\ 0 & 0 & e^{-i(2m+1)\pi} & 0 \\ 0 & 0 & 0 & e^{-i2(m+n+1)\pi} \end{pmatrix}. \tag{5.11}$$

This nothing but the gate in Eq. (5.7) thus the n.n. CZ gate is successfully applied to the logical qubits. It is straightforward and convenient to implement in the lab since this setting implies that just adjustment of the local potentials and the n.n. interaction strength are required for performing the n.n. CZ gate. Here time t is ignored in the unitary since it does nothing but uniformly shifts values of parameters in the Hamiltonian, thus the criteria in Eq. (5.10) becomes:

$$-\mu_2 = \frac{(2m+1)\pi}{t}, -\mu_3 = \frac{2n\pi}{t}, \lambda = \frac{(2l+1)\pi}{t}. \tag{5.12}$$

The presence of n.n. interaction is indeed the very thing that breaks the matchgate formalism. However, it is quite interesting that if we set the interaction λ to be $\lambda = 2l\pi$, it turns out that the generated quantum gate still remains a matchgate. This means that fermions with n.n. interactions that take even number of π are also classically efficiently simulatable. Hence, the $\lambda = 2l\pi$ case can be regarded as the generalization of classically efficient simulation of non-interacting fermions to interacting fermions. Moreover, if time is

included in the unitary $e^{-iH^{(2)}_{\rm tot}t}$, the criterion for classical efficient simulation of interacting fermions becomes $\lambda = \frac{2l\pi}{t}$, allowing more values of λ to be taken due to the shift from time t.

Therefore, interacting fermions under the evolution governed by the Hamiltonian in Eq. (5.8), with a judicious setting of parameters, can perform universal quantum computation. This proposal features turning on and off the tunneling amplitudes inside double-wells and turning off and on the n.n. interactions between wells. The former is accomplished by changing the power in the lasers that form the double-well lattice and the later might be accomplished using dipole-dipole interactions with the application of a local electric field. Additionally, the read-out of the output state can be carried out via measuring the spatial modes, i.e. to determine which site a fermion sits in. The imaging and position measurement of fermionic atoms, such as ^{40}K and ^{6}Li were already successfully achieved in the laboratory [45–48]. However, it is still quite challenging to implement this model in the laboratory due to the difficultly of turning on and off the interactions, which is one of the main drawbacks to this n.n. interaction proposal. Thus, it is reasonable to explore a more tractable physical model to see if we are able to achieve UQC under more experimentally realizable conditions. The following section attempts to address this issue by exploring the well-known Hubbard model to construct a universal set of quantum gates.

5.2 Universal quantum computation with Hubbard model

This section discusses the possibility of achieving UQC based on the Hubbard model, which so far may be the physical model that has simplest form for describing interacting fermions and is also implementable in the lab [44] but it is still very challenging to achieve sufficiently low temperature for which this model is a good approximation. Previously, I demonstrated that UQC is possible with spinless interacting fermions with n.n. interactions that break the formalism of matchgate. In this section, I start by showing the formalism for spin-1/2

fermions, then I introduce on-site interactions, and finally present the realization of two-qubit entangling gates based on the Hubbard model. The potential implementation of this scheme with current experimental techniques on ultracold atomic gases would be discussed in Chapter 6.

5.2.1 Extending matchgates to spin-1/2 fermions

Since the spin degree of freedom is allowed in the system, the non-interacting Hamiltonian for spin-1/2 fermions becomes:

$$\hat{H}_{\mathrm{hop},\sigma} = -\sum_{\langle i,j\rangle,\sigma} (t_{i\sigma j\sigma} a^{\dagger}_{i\sigma} a_{j\sigma} + H.c) - \sum_{i,\sigma} \mu_{i\sigma} a^{\dagger}_{i\sigma} a_{i\sigma}. \tag{5.13}$$

The first term stands for the n.n. hopping for spin-up and spin-down fermions separately. One may impose that the hopping strengths for different spins are the same but let us keep it more general by labeling them differently. The second term represents the local potential, and again we allow a more generic expression via labeling local potentials with spin σ. Because we intend to explore the Hamiltonian within the context of the Hubbard model, spin flips are not allowed in the system, i.e. both the spin projection and number of fermions are preserved.

In Sec. 4.3, it was shown that the evolution of spin-polarized non-interacting fermions can be mapped to matchgates. Let us now investigate this generalized Hamiltonian to see if it is also equivalent to the formalism of matchgate. Consider the two-mode Hamiltonian:

$$\hat{H}^{(2)}_{\mathrm{hop},\sigma} = -\sum_{\sigma} (t_{1\sigma 2\sigma} a^{\dagger}_{1\sigma} a_{2\sigma} + H.c) - \mu_{1\sigma} a^{\dagger}_{1\sigma} a_{1\sigma} - \mu_{2\sigma} a^{\dagger}_{2\sigma} a_{2\sigma}. \tag{5.14}$$

Based on this Hamiltonian, the complete basis is 16-dimensional so that we can write this Hamiltonian as a 16×16 matrix, analogously to the 4×4 one discussed in Sec. 4.3. Furthermore, due to the number-preservation, this Hamiltonian can be written as a direct sum of Hamiltonians with different total particle number:

$$H^{(2)}_{\mathrm{hop},\sigma} = H_0 \oplus H_1 \oplus H_2 \oplus H_3 \oplus H_4, \tag{5.15}$$

where H_k corresponds to the k-particle Hamiltonian. The dimensions of these Hamiltonians depend on the number of possible particles in each case. Therefore, the Hamiltonian $H^{(2)}_{\text{hop},\sigma}$ becomes:

$$H^{(2)}_{\text{hop},\sigma} = \begin{pmatrix} H_0 & & & & \\ & H_1 & & & \\ & & H_2 & & \\ & & & H_3 & \\ & & & & H_4 \end{pmatrix} \tag{5.16}$$

where the empty elements are zero. They take the following forms:

$$H_0 = 0$$

$$H_1 = \begin{pmatrix} -\mu_{1\uparrow} & -t_{1\uparrow 2\uparrow} & 0 & 0 \\ -t_{2\uparrow 1\uparrow} & -\mu_{2\uparrow} & 0 & 0 \\ 0 & 0 & -\mu_{1\downarrow} & -t_{1\downarrow 2\downarrow} \\ 0 & 0 & -t_{2\downarrow 1\downarrow} & -\mu_{2\downarrow} \end{pmatrix} \begin{matrix} |1\uparrow\rangle \\ |2\uparrow\rangle \\ |1\downarrow\rangle \\ |2\downarrow\rangle \end{matrix}$$

$$H_2 = \begin{pmatrix} -\mu_{1\uparrow}-\mu_{1\downarrow} & 0 & -t_{1\downarrow 2\downarrow} & -t_{1\uparrow 2\uparrow} & 0 & 0 \\ 0 & -\mu_{1\uparrow}-\mu_{2\uparrow} & 0 & 0 & 0 & 0 \\ -t_{2\downarrow 1\downarrow} & 0 & -\mu_{1\uparrow}-\mu_{2\downarrow} & 0 & 0 & -t_{1\uparrow 2\uparrow} \\ -t_{2\uparrow 1\uparrow} & 0 & 0 & -\mu_{1\downarrow}-\mu_{2\uparrow} & 0 & -t_{1\downarrow 2\downarrow} \\ 0 & 0 & 0 & 0 & -\mu_{1\downarrow}-\mu_{2\downarrow} & 0 \\ 0 & 0 & -t_{2\uparrow 1\uparrow} & -t_{2\downarrow 1\downarrow} & 0 & -\mu_{2\uparrow}-\mu_{2\downarrow} \end{pmatrix} \begin{matrix} |1\uparrow 1\downarrow\rangle \\ |1\uparrow 2\uparrow\rangle \\ |1\uparrow 2\downarrow\rangle \\ |2\uparrow 1\downarrow\rangle \\ |1\downarrow 2\downarrow\rangle \\ |2\uparrow 2\downarrow\rangle \end{matrix} \tag{5.17}$$

$$H_3 = \begin{pmatrix} -\mu_{1\uparrow}-\mu_{1\downarrow}-\mu_{2\uparrow} & 0 & -t_{1\downarrow 2\downarrow} & 0 \\ 0 & -\mu_{1\uparrow}-\mu_{1\downarrow}-\mu_{2\downarrow} & 0 & -t_{1\uparrow 2\uparrow} \\ -t_{2\downarrow 1\downarrow} & 0 & -\mu_{1\uparrow}-\mu_{2\uparrow}-\mu_{2\downarrow} & 0 \\ 0 & -t_{2\uparrow 1\uparrow} & 0 & -\mu_{1\downarrow}-\mu_{2\uparrow}-\mu_{2\downarrow} \end{pmatrix} \begin{matrix} |1\uparrow 2\uparrow 1\downarrow\rangle \\ |1\uparrow 1\downarrow 2\downarrow\rangle \\ |1\uparrow 2\uparrow 2\downarrow\rangle \\ |2\uparrow 1\downarrow 2\downarrow\rangle \end{matrix}$$

$$H_4 = (-\mu_{1\uparrow}-\mu_{2\uparrow}-\mu_{1\downarrow}-\mu_{2\downarrow}). \quad |1\uparrow 2\uparrow 1\downarrow 2\downarrow\rangle$$

If the evolution under this Hamiltonian can also be mapped to the matchgate formalism, the unitary $U_{\text{hop},\sigma} = e^{-iH^{(2)}_{\text{hop},\sigma}}$ [1] must be written as a tensor product of two matchgates; that is:

$$U_{\text{hop},\sigma} = e^{-iH^{(2)}_{\text{hop},\sigma}} \stackrel{?}{=} G_\uparrow \otimes G_\downarrow, \tag{5.18}$$

where G_σ corresponds to the matchgate associated with spin σ. This is equivalent to showing that the Hamiltonian $H^{(2)}_{\text{hop},\sigma}$ can be written as the Cartesian product:

$$H_\uparrow \otimes I_\downarrow + I_\uparrow \otimes H_\downarrow \tag{5.19}$$

[1] The evolution time t is ignored here because it just globally shifts all parameters in the Hamiltonian.

which ensures

$$G_\uparrow = e^{-iH_\uparrow}, G_\downarrow = e^{-iH_\downarrow}. \tag{5.20}$$

First, let us write out the specific form of $H_\uparrow \otimes I_\downarrow$ and $I_\uparrow \otimes H_\downarrow$

$$H_\uparrow \otimes I_\downarrow = \begin{pmatrix} 0 & 0 & 0 & 0 \\ 0 & -\mu_{1\uparrow} & -t_{1\uparrow 2\uparrow} & 0 \\ 0 & -t_{2\uparrow 1\uparrow} & -\mu_{2\uparrow} & 0 \\ 0 & 0 & 0 & -\mu_{1\uparrow} - \mu_{2\uparrow} \end{pmatrix} \otimes \begin{pmatrix} 1 & 0 & 0 & 0 \\ 0 & 1 & 0 & 0 \\ 0 & 0 & 1 & 0 \\ 0 & 0 & 0 & 1 \end{pmatrix} \tag{5.21}$$

and

$$I_\uparrow \otimes H_\downarrow = \begin{pmatrix} 1 & 0 & 0 & 0 \\ 0 & 1 & 0 & 0 \\ 0 & 0 & 1 & 0 \\ 0 & 0 & 0 & 1 \end{pmatrix} \otimes \begin{pmatrix} 0 & 0 & 0 & 0 \\ 0 & -\mu_{1\downarrow} & -t_{1\downarrow 2\downarrow} & 0 \\ 0 & -t_{2\downarrow 1\downarrow} & -\mu_{2\downarrow} & 0 \\ 0 & 0 & 0 & -\mu_{1\downarrow} - \mu_{2\downarrow} \end{pmatrix}. \tag{5.22}$$

With these matrices, we are able to compare the matrix $H_\uparrow \otimes I_\downarrow + I_\uparrow \otimes H_\downarrow$ to the matrix in the Eq. (5.16). Expectedly, they end up being the same. In hindsight, the Hamiltonian $H^{(2)}_{\mathrm{hop},\sigma}$ is separable spin-wise because the Eq. (5.14) already implies that it is non-interacting spin-wise, thus two spin channels must be independent. Hence, the evolution of spin-1/2 non-interacting fermions can also be mapped to matchgates associated with spin σ, which can be efficiently simulated on a classical computer.

5.2.2 On-site interactions

Let us now investigate what happens if an on-site interaction is added. The two-mode Hamiltonian becomes:

$$\hat{H}^{(2)}_{\mathrm{tot},\sigma} = \hat{H}^{(2)}_{\mathrm{hop},\sigma} + g \sum_{i=1}^{2} a^\dagger_{i\uparrow} a_{i\uparrow} a^\dagger_{i\downarrow} a_{i\downarrow}, \tag{5.23}$$

where g is the on-site interaction strength. Similar to the non-interacting case, we can write this Hamiltonian in two 16×16 matrices corresponding to the hopping term and the on-site interaction term:

$$H^{(2)}_{\mathrm{tot},\sigma} = H^{(2)}_{\mathrm{hop},\sigma} + H^{(2)}_{\mathrm{int},\sigma}, \tag{5.24}$$

where $H^{(2)}_{\text{int},\sigma}$ takes the following form:

$$H^{(2)}_{\text{int},\sigma} = \begin{pmatrix} H_{\text{int}_0} & & & & \\ & H_{\text{int}_1} & & & \\ & & H_{\text{int}_2} & & \\ & & & H_{\text{int}_3} & \\ & & & & H_{\text{int}_4} \end{pmatrix} \tag{5.25}$$

where the empty elements are zero and H_{int_k} represents the k-particle on-site interaction Hamiltonian. They take forms as follows:

$$\begin{aligned} H_{\text{int}_0} &= 0 \\ H_{\text{int}_1} &= \begin{pmatrix} 0 & 0 & 0 & 0 \\ 0 & 0 & 0 & 0 \\ 0 & 0 & 0 & 0 \\ 0 & 0 & 0 & 0 \end{pmatrix} \begin{matrix} |1\uparrow\rangle \\ |2\uparrow\rangle \\ |1\downarrow\rangle \\ |2\downarrow\rangle \end{matrix} \\ H_{\text{int}_2} &= \begin{pmatrix} g & 0 & 0 & 0 & 0 & 0 \\ 0 & 0 & 0 & 0 & 0 & 0 \\ 0 & 0 & 0 & 0 & 0 & 0 \\ 0 & 0 & 0 & 0 & 0 & 0 \\ 0 & 0 & 0 & 0 & 0 & 0 \\ 0 & 0 & 0 & 0 & 0 & g \end{pmatrix} \begin{matrix} |1\uparrow 1\downarrow\rangle \\ |1\uparrow 2\uparrow\rangle \\ |1\uparrow 2\downarrow\rangle \\ |2\uparrow 1\downarrow\rangle \\ |1\downarrow 2\downarrow\rangle \\ |2\uparrow 2\downarrow\rangle \end{matrix} \\ H_{\text{int}_3} &= \begin{pmatrix} g & 0 & 0 & 0 \\ 0 & g & 0 & 0 \\ 0 & 0 & g & 0 \\ 0 & 0 & 0 & g \end{pmatrix} \begin{matrix} |1\uparrow 2\uparrow 1\downarrow\rangle \\ |1\uparrow 1\downarrow 2\downarrow\rangle \\ |1\uparrow 2\uparrow 2\downarrow\rangle \\ |2\uparrow 1\downarrow 2\downarrow\rangle \end{matrix} \\ H_{\text{int}_4} &= 2g. \quad |1\uparrow 2\uparrow 1\downarrow 2\downarrow\rangle \end{aligned} \tag{5.26}$$

The proof of separability is the same as the non-interacting one. It is known that $H^{(2)}_{\text{hop},\sigma}$ can be factorized as $H_\uparrow \otimes I_\downarrow + I_\uparrow \otimes H_\downarrow$ so if $H^{(2)}_{\text{tot},\sigma} = H^{(2)}_{\text{hop},\sigma} + H^{(2)}_{\text{int},\sigma}$ can also be likewise factorized then:

$$H^{(2)}_{\text{tot},\sigma} \stackrel{?}{=} H'_\uparrow \otimes I_\downarrow + I_\uparrow \otimes H'_\downarrow. \tag{5.27}$$

then the interaction Hamiltonian $H^{(2)}_{\text{int},\sigma}$ must then be written as:

$$H^{(2)}_{\text{int}} = H''_\uparrow \otimes I_\downarrow + I_\uparrow \otimes H''_\downarrow, \tag{5.28}$$

where $H''_\uparrow = H'_\uparrow - H_\uparrow$ and $H''_\downarrow = H'_\downarrow - H_\downarrow$.

Because we expect them to have the formalism of matchgate, we can assume that $H''_\uparrow$ and $H''_\downarrow$ have the following form:

$$\begin{aligned} H''_\uparrow &= \begin{pmatrix} 0 & 0 & 0 & 0 \\ 0 & k_1 & k_2 & 0 \\ 0 & k_2 & k_3 & 0 \\ 0 & 0 & 0 & k_1 + k_3 \end{pmatrix} \\ H''_\downarrow &= \begin{pmatrix} 0 & 0 & 0 & 0 \\ 0 & k'_1 & k'_2 & 0 \\ 0 & k'_2 & k'_3 & 0 \\ 0 & 0 & 0 & k'_1 + k'_3 \end{pmatrix} \end{aligned}. \tag{5.29}$$

Then, one needs to plug these back into Eq. (5.28), permutes the order of all input states to match with the matrix in Eq. (5.25), and solve all the parameters in matrices $H''_\uparrow$ and $H''_\downarrow$ for any real number g. It turns out that the only solution corresponds to $g = 0$, otherwise all other parameters are 0. This means with on-site interactions, it is not possible to write the Hamiltonian $H^{(2)}_{\text{tot},\sigma} = H^{(2)}_{\text{hop},\sigma} + H^{(2)}_{\text{int},\sigma}$ as in the Cartesian product form. Hence, we can claim:

$$e^{-iH^{(2)}_{\text{tot},\sigma}} = e^{-i(H^{(2)}_{\text{hop},\sigma} + H^{(2)}_{\text{int},\sigma})} \neq G'_\uparrow \otimes G'_\downarrow, \tag{5.30}$$

where $G'_\uparrow = e^{-iH'_\uparrow}, G_\downarrow = e^{-iH'_\downarrow}$.

As the on-site interaction breaks the formalism of matchgate, the Hamiltonian with hopping and an on-site interaction may have the power to elevate matchgate circuits to universal quantum circuits:

$$\hat{H}_{\text{Hubbard}} = -\sum_{\langle i,j\rangle,\sigma} (t_{i\sigma j\sigma} a^\dagger_{i\sigma} a_{j\sigma} + H.c) - \sum_{i,\sigma} \mu_{i\sigma} a^\dagger_{i\sigma} a_{i\sigma} + g \sum_i \hat{n}_{i\uparrow} \hat{n}_{i\downarrow}. \tag{5.31}$$

This Hamiltonian is within the family of the Hubbard models but it allows for the variation of the local potential and the hopping strength. The following sections are focused on implementing single-qubit and two-qubit gates based on this model.

5.2.3 Single-qubit gates

Before proceeding to the qubit operation, it is important to define the encoding scheme used to define qubits. Inspired by the encoding scheme employed in Sec. 5.1, we take the following encoding:

$$\begin{aligned} |0\rangle_L = |1\uparrow\rangle, |1\rangle_L = |2\uparrow\rangle, \\ |0'\rangle_L = |3\downarrow\rangle, |1'\rangle_L = |4\downarrow\rangle, \end{aligned} \tag{5.32}$$

where th numbers 1 through 4 are the site number in lattice and L stands for 'logical.' This encoding indicates that the lattice is quarter-filled: sites 1 and 2 share one spin-up particle, and sites 3 and 4 share one spin-down particle. In Fig. 5.2, one can see that with this encoding, the lattice is alternatively filled with spin-up and spin-down fermions every two sites. Moreover, like the spin-polarized case, high potential walls between double-wells prevent hopping between different double-wells in order to avoid disruption in the encoding scheme. The corresponding Hamiltonian can be written as:

$$\hat{H}_{\text{spin-dep}} = -\sum_{i,\sigma} (t_{2i-1\sigma,2i\sigma} a^\dagger_{2i-1\sigma} a_{2i\sigma} + \tilde{t}_{2i\sigma,2i+1\sigma} a^\dagger_{2i\sigma} a_{2i+1\sigma} + H.c) - \sum_{i,\sigma} \mu_{i\sigma} a^\dagger_{i\sigma} a_{i\sigma} + g \sum_i n_{i\uparrow} n_{i\downarrow} \tag{5.33}$$

where $\tilde{t}_{2i\sigma,2i+1\sigma}$ is the hopping amplitude between well for different spins, and $t_{2i-1\sigma,2i\sigma}$ is the hopping amplitude inside wells. The relative strength between them depends on the quantum gates that one desires to implement. $-\mu_{i\sigma}$ is the local potential at each site, dependent on spin. Given that the hopping is only within a single double-well, the single-qubit gates are implemented in precisely the same way as for the spinless (spin-polarized)[2] example treated in Sec. 5.1.1.

Based on this encoding, the single-qubit rotations can be applied to spin-up or spin-down fermions individually via adjusting local potentials and the intra-well hopping strength. Since the lattice is quarter-filled, the 16×16 two-mode Hamiltonian is simplified to the follows:

$$\begin{pmatrix} -\mu_{1\uparrow} & -t_{1\uparrow 2\uparrow} \\ -t_{2\uparrow 1\uparrow} & -\mu_{2\uparrow} \end{pmatrix} \tag{5.34}$$

[2]This means the spin is aligned (fixed) with a given direction by the application of a magnetic field.

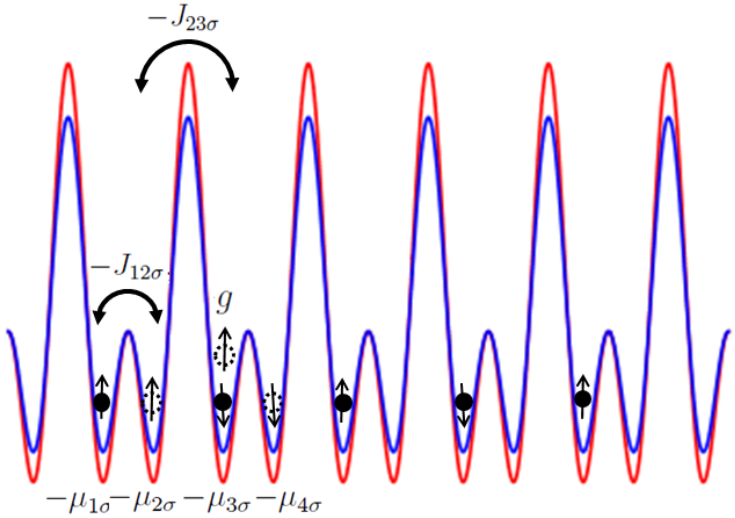

Figure 5.2: The figure shows the physical lattice that we use to perform single-qubit and two-qubit gates, especially the CZ gate to achieve UQC. The lattice is spin-dependent so we are able to adjust all parameters in the system separately for spin-up and down fermions and it is eligible for implementing UQC via adjusting the hopping strength $-J_{\langle i,j\rangle\sigma}$, the local potential $-\mu_{i\sigma}$ and the on-site interaction strength g with time t.

where $\uparrow$ stands for spin up and $-t_{1\uparrow 2\uparrow} = -t_{2\uparrow 1\uparrow} = -J_{12\uparrow}$ represents the hopping strength between sites 1 and 2 for spin-up fermion and $-\mu_{1\uparrow}, -\mu_{2\uparrow}$ are local potentials at sites 1 and 2. In addition, for the spin-down fermion encoded on site 3 and 4, the Hamiltonian becomes:

$$\begin{pmatrix} -\mu_{3\downarrow} & -t_{3\downarrow 4\downarrow} \\ -t_{4\downarrow 3\downarrow} & -\mu_{4\downarrow} \end{pmatrix} \tag{5.35}$$

where $\downarrow$ stands for spin down and $-t_{3\downarrow 4\downarrow} = -t_{4\downarrow 3\uparrow} = -J_{34\downarrow}$ represent the hopping strength between site 3 and 4 for spin-down fermion and $-\mu_{3\downarrow}, -\mu_{4\downarrow}$ are local potentials at sites 3 and 4. These two Hamiltonians are exactly the same as the one for spin-polarized case except that here all the parameters are spin-dependent. Likewise, we can rewrite them as:

$$\begin{aligned} &-J_{12\uparrow}X + \frac{-\mu_{1\uparrow}+\mu_{2\uparrow}}{2}Z + \frac{-\mu_{1\uparrow}-\mu_{2\uparrow}}{2}I \\ &-J_{34\downarrow}X + \frac{-\mu_{3\downarrow}+\mu_{4\downarrow}}{2}Z + \frac{-\mu_{3\downarrow}-\mu_{4\downarrow}}{2}I \end{aligned} \tag{5.36}$$

and recalling the arbitrary single-qubit gate, Eq. (5.5), we are capable of applying any one-qubit operation to two different types of qubit encoded in adjacent double-wells.

As all parameters are labeled with spin, the proposal requires the control of spin-up and spin-down fermions independently. This means that a spin-dependent lattice is in principle

required in the lab; however, using a spin-dependent lattice is not necessarily required to achieve single-qubit operations because our qubits are encoded by their positions in every two sites in the lattice regardless of spins, as shown in Fig. 5.3. But in order to harness the power of on-site interactions, the spin degree of freedom must be included.

5.2.4 Two-qubit gates

In this section, I will first discuss how to construct two-qubit entangling gates in the spin-independent lattice, but we shall see that it fails to yield an entangling gate that can be used for UQC. Then, I will turn to spin-dependent lattice, showing that it is eligible to achieve two-qubit entangling gates, and discuss the potential of implementing this scheme in the lab using current techniques.

5.2.4.1 Spin-independent lattice for two-qubit gates

Let us first investigate constructing a two-qubit entangling gate in a spin-independent lattice, as shown in Fig. 5.3. Unlike the spin-polarized case where n.n. interaction is introduced to entangle two n.n. qubits, which is quite straightforward at least theoretically, here in the spin-1/2 system, we consider the more physically motivated on-site interaction between particles of different spin, thus giving us hope to make an entangling gate. However, in order to utilize the on-site interaction, we must allow hopping between two spin-up and spin-down fermions in adjacent double-wells that are separated by the high potential wall. This could immediately causes a serious problem: the encoding of quantum information in the system would be disrupted if these two qubits fail to hop back to their previous positions. This is a constraint of our scheme that needs to be satisfied.

The approach to generate an entangling gate between two n.n. fermionic qubits works as follows: turn on the hopping between these two qubits for a certain amount of time, during which they pick up a phase and also return to where they start. That is to say, we aim at

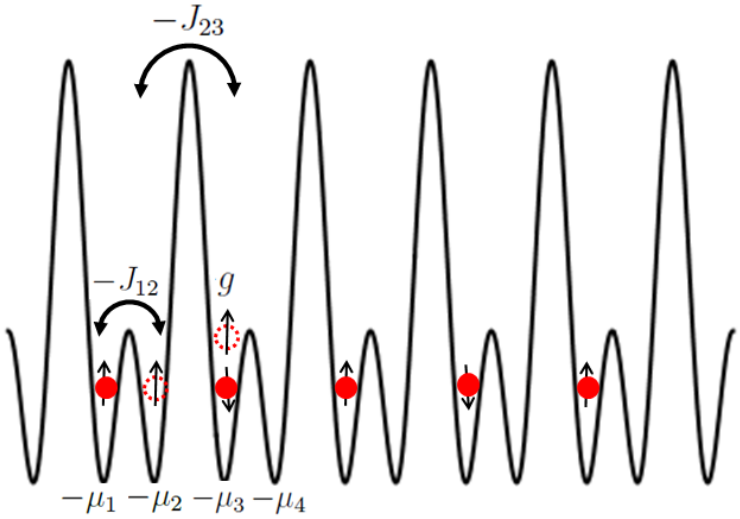

Figure 5.3: The spin-independent lattice configuration for implementing UQC. All the parameters in the system see spin-up and down fermions indiscriminately and it is just eligible for performing single-qubit rotations via adjusting the hopping strength $-J_{\langle i,j\rangle}$, the local potential $-\mu_i$ but fails to achieve two-qubit entangling gates

the following mapping:

$$(\alpha\,|1\uparrow\rangle+\beta\,|2\uparrow\rangle)(\gamma\,|3\downarrow\rangle+\delta\,|4\downarrow\rangle)\rightarrow\alpha\gamma\,|1\uparrow 3\downarrow\rangle+\alpha\delta\,|1\uparrow 4\downarrow\rangle+\beta\gamma e^{i\theta}\,|2\uparrow 3\downarrow\rangle+\beta\delta\,|2\uparrow 4\downarrow\rangle\,, \tag{5.37}$$

where the phase $e^{i\theta}$ arises from this process and as long as $\theta\neq 2\pi n$, this two-qubit state must be entangled. Actually the phase could be located on any of the terms for the gate to be entangling; for the moment, we just aim at implementing a phase gate but the CZ gate is literally what we prefer to implement due to its low cost to generate the SWAP gate. This mapping in our encoding is equivalent to:

$$(\alpha\,|0\rangle_L+\beta\,|1\rangle_L)(\gamma\,|0'\rangle_L+\delta\,|1'\rangle_L)\rightarrow\alpha\gamma\,|00'\rangle_L+\alpha\delta\,|01'\rangle_L+\beta\gamma e^{i\theta}\,|10'\rangle_L+\beta\delta\,|11'\rangle_L\,. \tag{5.38}$$

Because the on-site interaction happens at site 2 and 3, a phase could only be directly generated on the state $|10'\rangle_L$. It imposes no problem at all as it is a regular phase gate just

up to some local rotations, for instance the CZ gate

$$\begin{pmatrix} 1 & 0 & 0 & 0 \\ 0 & 1 & 0 & 0 \\ 0 & 0 & -1 & 0 \\ 0 & 0 & 0 & 1 \end{pmatrix} = (I \otimes X)\mathrm{CZ}(I \otimes X). \tag{5.39}$$

Eq. (5.33) is the Hamiltonian for the Hubbard model in the spin-dependent lattice whereas the general Hamiltonian for a spin-independent lattice should be:

$$\hat{H}_{\text{spin-indep}} = -\sum_{i,\sigma} (t_{2i-1,2i} a^\dagger_{2i-1\sigma} a_{2i\sigma} + \tilde{t}_{2i,2i+1} a^\dagger_{2i\sigma} a_{2i+1\sigma} + H.c) - \sum_{i,\sigma} \mu_i a^\dagger_{i\sigma} a_{i\sigma} + g \sum_i n_{i\uparrow} n_{i\downarrow}, \tag{5.40}$$

where $\tilde{t}_{2i,2i+1}$ is the hopping amplitude between double-wells for different spins, which here is much stronger than the hopping $t_{2i-1,2i}$ inside wells, and $-\mu_i$ is the local potential at each site. Distinct from Eq. (5.33), all parameters here are independent of spin σ, thus the suppression of the spin index on the hopping amplitudes and the local potential. As the gate should be implemented on the crossover lines of these two qubits, we just consider the Hamiltonian in the context of sites 2 and 3 only. Before writing it out, let us take a close look at the general two-qubit state:

$$\underbrace{\alpha\gamma\,|1\uparrow 3\downarrow\rangle}_{\text{one-body}} + \underbrace{\alpha\delta\,|1\uparrow 4\downarrow\rangle}_{\text{vacuum}} + \underbrace{\beta\gamma\,|2\uparrow 3\downarrow\rangle}_{\textbf{two-body}} + \underbrace{\beta\delta\,|2\uparrow 4\downarrow\rangle}_{\text{one-body}}, \tag{5.41}$$

where we have three types of quantum states because the gate only acts on site 2 and 3 which results in various input sizes for different terms. Physically, it indicates that the hopping between site 1 and 2 and site 3 and 4 must be turned off during this process, accomplished by increasing the barrier between sites 1 and 2, and between 3 and 4, while simultaneously lowering the barrier between 2 and 3. In matrix form, this Hamiltonian is written as:

$$H^{(2)}_{SI} = \begin{pmatrix} H_{\text{vac}} & & \\ & H_{\text{one-body}} & \\ & & H_{\text{two-body}} \end{pmatrix} \tag{5.42}$$

where all these submatrices take the following forms:

$$
\begin{aligned}
H_{\text{vac}} &= 0 \\
H_{\text{one-body}} &= \begin{pmatrix} -\mu_2 & -J_{23} & 0 & 0 \\ -J_{23} & -\mu_3 & 0 & 0 \\ 0 & 0 & -\mu_2 & -J_{23} \\ 0 & 0 & -J_{23} & -\mu_3 \end{pmatrix} \begin{matrix} |2\uparrow\rangle \\ |3\uparrow\rangle \\ |2\downarrow\rangle \\ |3\downarrow\rangle \end{matrix} \\
H_{\text{two-body}} &= \begin{pmatrix} -2\mu_2+g & -J_{23} & -J_{23} & 0 \\ -J_{23} & -\mu_2-\mu_3 & 0 & -J_{23} \\ -J_{23} & 0 & -\mu_2-\mu_3 & -J_{23} \\ 0 & -J_{23} & -J_{23} & -2\mu_3+g \end{pmatrix} \begin{matrix} |2\uparrow 2\downarrow\rangle \\ |2\uparrow 3\downarrow\rangle \\ |3\uparrow 2\downarrow\rangle \\ |3\uparrow 3\downarrow\rangle \end{matrix}
\end{aligned}
\tag{5.43}
$$

where $-\tilde{t}_{23} = -\tilde{t}_{32} = -J_{23}$ is the hopping amplitude for spin-up and down fermions at site 2 and 3 and vac is the vacuum. With these Hamiltonians in hand, we are able to investigate how to construct an entangling gate.

The input quantum state, i.e. Eq. (5.41), requires the total evolution to apply the identity to the two blocks of the vacuum and one-body matrices but a nontrivial phase to the two-body term. Let us start with the unitary $e^{-iH_{\text{vac}}t}$; for vacuum-like terms the Hamiltonian is always $H_{\text{vac}} = 0$, which results in the unitary $U_{\text{vac}} = I$. Because two submatrices in $H_{\text{one-body}}$ are exactly the same for spin-up and spin-down particles at sites 2 and 3, we just need to study one of them, hence reducing this 4×4 matrix to a 2×2 matrix. In order to simplify the calculation, the J_{23} is chosen to as the energy scale, then the one-body unitary becomes:

$$
U_{\text{one-body}} = e^{-iH_{\text{one-body}}t} = e^{-i\left(\begin{smallmatrix} -\mu_2 & -1 \\ -1 & -\mu_3 \end{smallmatrix}\right)t}. \tag{5.44}
$$

where $-\mu_2, -\mu_3$ and t are not original parameters but are parameters that scale with J_{23}. The following criteria are found, when we have $U_{\text{one-body}} = I$:

$$
t = \frac{2\pi}{\sqrt{(-\mu_2+\mu_3)^2+4}}, \quad \mu_3 = \frac{1}{\mu_2}. \tag{5.45}
$$

Plugging these into the two-body Hamiltonian $H_{\text{two-body}}$, we end up obtaining:

$$H_{\text{two-body}} = \begin{pmatrix} -2\mu_2 + g & -1 & -1 & 0 \\ -1 & -\mu_2 + \frac{1}{-\mu_2} & 0 & -1 \\ -1 & 0 & -\mu_2 + \frac{1}{-\mu_2} & -1 \\ 0 & -1 & -1 & \frac{2}{-\mu_2} + g \end{pmatrix} \tag{5.46}$$

which gives us the unitary $U_{\text{two-body}} = e^{-iH_{\text{two-body}}t}$, where t is given by the one-body constraint above governing the evolution. Actually, our target is just the (2,2) element of the unitary due to the fact that it is only the two-body input in Eq. (5.41) that is relevant to the entangling gate. The goal is to make this matrix element of the unitary derived from Eq. (5.46) a certain phase $e^{i\theta}$ via adjusting the parameters $-\mu_2$ and g.

The full analytical calculation is very cumbersome so instead we choose to perform a numerical analysis. The numerical results can be found in the Appendix A, from which it is clear that the only case where the amplitiude of the (2,2) matrix element is unity gives zero phase. This means that enforcing the constraint that there is no leakage of the original encoded quantum information, no entanglement between these two qubits is possible no matter how we adjust parameters in the system. Whenever the amplitude of the (2,2) element is preserved, the on-site interaction g is always zero which brings us back to the non-interacting case.

The restriction that both phases for one-body terms are zero is perhaps too strong. Instead suppose that these phases will all conspire to give us an entangling gate. With the same time $t = \frac{2\pi}{\sqrt{4+(-\mu_2+\mu_3)^2}}$ the one-body unitary $U_{\text{one-body}}$ becomes:

$$U_{\text{one-body}} = \begin{pmatrix} -e^{-i\frac{\pi(-\mu_2-\mu_3)}{\sqrt{4+(-\mu_2+\mu_3)^2}}} & 0 \\ 0 & -e^{-i\frac{\pi(\mu_2-\mu_3)}{\sqrt{4+(-\mu_2+\mu_3)^2}}} \end{pmatrix} \tag{5.47}$$

which still preserves the unity of one-body terms. While keeping these phases, we also numerically analyze $U_{\text{two-body}}$ (note that the relationship between $-\mu_2$ and $-\mu_3$ in Eq. (5.45) longer holds) and unfortunately, the same conclusion is reached: the only cases where the amplitude on the (2,2) matrix element is unity correspond to $g = 0$, resulting in the failure

to make an entangling gate. This can easily understood; these remaining phases from the one-body terms can be generated only by controlling the local potentials at sites 2 and 3 (this is clear from the dependence of the unitary, Eq. (5.47), on μ_2 and μ_3), which obviously has no power to entangle qubits because entanglement is impervious to single-particle operations. In the light of the fact that local operations fail to generate the entanglement, the full analytical calculation can be simplified to just cope with the following Hamiltonians:

$$
\begin{aligned}
&H_{\text{vac}} = 0 \\
&\tilde{H}_{\text{one-body}} = \begin{pmatrix} 0 & -J_{23} & 0 & 0 \\ -J_{23} & 0 & 0 & 0 \\ 0 & 0 & 0 & -J_{23} \\ 0 & 0 & -J_{23} & 0 \end{pmatrix} \begin{matrix} |2\uparrow\rangle \\ |3\uparrow\rangle \\ |2\downarrow\rangle \\ |3\downarrow\rangle \end{matrix} \\
&\tilde{H}_{\text{two-body}} = \begin{pmatrix} g & -J_{23} & -J_{23} & 0 \\ -J_{23} & 0 & 0 & -J_{23} \\ -J_{23} & 0 & 0 & -J_{23} \\ 0 & -J_{23} & -J_{23} & g \end{pmatrix} \begin{matrix} |2\uparrow 2\downarrow\rangle \\ |2\uparrow 3\downarrow\rangle \\ |3\uparrow 2\downarrow\rangle \\ |3\uparrow 3\downarrow\rangle \end{matrix}
\end{aligned}
\tag{5.48}
$$

That is to say, all the local potentials are turned off. In this case, the evolution time is found to be π using Eq. (5.45). Plugging this time into the two-body unitary $\tilde{U}_{\text{two-body}} = e^{-i\tilde{H}_{\text{two-body}}t}$ for calculating its (2,2) element, one obtains

$$
\tilde{U}(2,2) = \frac{e^{-\frac{1}{2}i(g+\sqrt{16+g^2})\pi}\big((-1+e^{i\sqrt{16+g^2}\pi})g + (1+e^{i\sqrt{16+g^2}\pi} + 2e^{\frac{1}{2}i(g+\sqrt{16+g^2})\pi})\sqrt{16+g^2}\big)}{4\sqrt{16+g^2}}.
\tag{5.49}
$$

Our goal is to make this entry a phase. One can note that this is true only when the following criteria are satisfied:

$$
e^{i\sqrt{16+g^2}\pi} = 1, \quad e^{\frac{i}{2}(g+\sqrt{16+g^2})\pi} = 1. \tag{5.50}
$$

However, when these equations hold, we end up obtaining the phase $e^{-\frac{i}{2}(g+\sqrt{16+g^2})\pi}$, which is equal to 1. This agrees with the numerical calculation discussed above. If we further solve these two equations for the on-site interaction g, we find

$$
\frac{1}{2}(g+\sqrt{16+g^2}) = 2m, \ \sqrt{16+g^2} = 2n, \ m,n \in \mathbb{Z}. \tag{5.51}
$$

Thus, the on-site interaction g is found to be:

$$g = 4m - 2n, \tag{5.52}$$

where the integers m, n satisfy $n = m + \frac{1}{m}$. The only solution here is that $m = 1, n = 2$, which gives us $g = 0$. Again, this analytical result agrees with the numerical result in the Appendix A.

So far, we have only considered the possibility of building an entangling gate from crossover lines of two qubits, i.e. sites 2 and 3 in the spin-independent lattice. Since the scheme above does not work, it is reasonable to simultaneously try turning on the hopping between sites 1 and 2 (or it could be sites 3 and 4 but they are symmetric so either is sufficient) to investigate the potential of generating entanglement between these two qubits. In this case, our two-qubit general state becomes:

$$\underbrace{\alpha\gamma\,|1\uparrow 3\downarrow\rangle}_{\textbf{two-body}} + \underbrace{\alpha\delta\,|1\uparrow 4\downarrow\rangle}_{\text{one-body}} + \underbrace{\beta\gamma\,|2\uparrow 3\downarrow\rangle}_{\textbf{two-body}} + \underbrace{\beta\delta\,|2\uparrow 4\downarrow\rangle}_{\text{one-body}}, \tag{5.53}$$

which is the same as the state in Eq. (5.41) but with different types of input because of the change in operational process. This also leads to different Hamiltonians corresponding to this process:

$$H'_{\text{one-body}} = \begin{pmatrix} -\mu_1 & -J_{12} & 0 & 0 & 0 & 0 \\ -J_{12} & -\mu_2 & -J_{23} & 0 & 0 & 0 \\ 0 & -J_{23} & -\mu_3 & 0 & 0 & 0 \\ 0 & 0 & 0 & -\mu_1 & -J_{12} & 0 \\ 0 & 0 & 0 & -J_{12} & -\mu_2 & -J_{23} \\ 0 & 0 & 0 & 0 & -J_{23} & -\mu_3 \end{pmatrix} \begin{matrix} |1\uparrow\rangle \\ |2\uparrow\rangle \\ |3\uparrow\rangle \\ |1\downarrow\rangle \\ |2\downarrow\rangle \\ |3\downarrow\rangle \end{matrix}$$

$$H'_{tb} = \begin{pmatrix} -\mu_1-\mu_3 & -J_{12} & -J_{23} & 0 & 0 & 0 & 0 & 0 & 0 \\ -J_{12} & \mu_2-\mu_3 & 0 & -J_{23} & -J_{23} & 0 & 0 & 0 & 0 \\ -J_{23} & 0 & -\mu_1-\mu_2 & -J_{12} & 0 & -J_{12} & 0 & 0 & 0 \\ 0 & -J_{23} & -J_{12} & -2\mu_2+g & 0 & 0 & -J_{12} & 0 & -J_{23} \\ 0 & -J_{23} & 0 & 0 & -2\mu_3+g & 0 & 0 & 0 & -J_{23} \\ 0 & 0 & -J_{12} & 0 & 0 & -2\mu_1+g & -J_{12} & 0 & 0 \\ 0 & 0 & 0 & -J_{12} & 0 & -J_{12} & -\mu_1-\mu_2 & -J_{23} & 0 \\ 0 & 0 & 0 & 0 & 0 & 0 & -J_{23} & -\mu_1-\mu_3 & -J_{12} \\ 0 & 0 & 0 & -J_{23} & -J_{23} & 0 & 0 & -J_{12} & -\mu_2-\mu_3 \end{pmatrix} \begin{matrix} |1\uparrow 3\downarrow\rangle \\ |2\uparrow 3\downarrow\rangle \\ |1\uparrow 2\downarrow\rangle \\ |2\uparrow 2\downarrow\rangle \\ |3\uparrow 3\downarrow\rangle \\ |1\uparrow 1\downarrow\rangle \\ |2\uparrow 1\downarrow\rangle \\ |3\uparrow 1\downarrow\rangle \\ |3\uparrow 2\downarrow\rangle \end{matrix} \tag{5.54}$$

The numerical results and discussions can be found in the Appendix B where the same outcome is obtained that this scheme also fails to generate entanglement.

There is another scenario that we have not considered yet, that is to make the hopping between 3 and 4 also accessible. Then, all the input terms become two-body and the similar calculations are done numerically as well. Unfortunately, the heavy restriction on the preservation of quantum information encoded in this quantum state also kills this possibility. Turning on more hoppings and local potentials inside double wells is simply implementing local operations, which gives us a hindsight that local operations are unable to generate any entanglement between two qubits.

5.2.4.2 Spin-dependent lattice for two-qubit gates

The results above indicate that a two-qubit entangling gate is impossible with the spin-independent lattice, so turning to the spin-dependent lattice is desirable. We also aim at Eq. (5.37) but the Hamiltonian should be the one in Eq. (5.31) which depends on the spin σ. Let us again write out the Hamiltonian corresponding to sites 2 and 3 that is responsible for the evolution of the general two-qubit quantum state, i.e. Eq. (5.41):

$$
\begin{aligned}
H'_{\text{vac}} &= 0 \\
H'_{\text{one-body}} &= \begin{pmatrix} -\mu_{2\uparrow} & -J_{23\uparrow} & 0 & 0 \\ -J_{23\uparrow} & -\mu_{3\uparrow} & 0 & 0 \\ 0 & 0 & -\mu_{2\downarrow} & -J_{23\downarrow} \\ 0 & 0 & -J_{23\downarrow} & -\mu_{3\downarrow} \end{pmatrix} \begin{matrix} |2\uparrow\rangle \\ |3\uparrow\rangle \\ |2\downarrow\rangle \\ |3\downarrow\rangle \end{matrix} \\
H'_{\text{two-body}} &= \begin{pmatrix} -\mu_{2\uparrow}-\mu_{2\downarrow}+g & -J_{23\downarrow} & -J_{23\uparrow} & 0 \\ -J_{23\downarrow} & -\mu_{2\uparrow}-\mu_{3\downarrow} & 0 & -J_{23\uparrow} \\ -J_{23\uparrow} & 0 & -\mu_{2\downarrow}-\mu_{3\uparrow} & -J_{23\downarrow} \\ 0 & -J_{23\uparrow} & -J_{23\downarrow} & -\mu_{3\uparrow}-\mu_{3\downarrow}+g \end{pmatrix} \begin{matrix} |2\uparrow 2\downarrow\rangle \\ |2\uparrow 3\downarrow\rangle \\ |3\uparrow 2\downarrow\rangle \\ |3\uparrow 3\downarrow\rangle \end{matrix}
\end{aligned}
\tag{5.55}
$$

where all the these parameters depend on the spin, giving us more degrees of freedom to adjust in the system as shown in Fig. 5.2. Because we are able to control the hopping

strengths between site 2 and 3 and local potentials at site 2 and 3 separately for spin $\uparrow$ and $\downarrow$, let's consider the simplest non-trivial configuration of parameters:

$$-J_{23\uparrow} = -\mu_{2\uparrow} = -\mu_{2\downarrow} = -\mu_{3\uparrow} = -\mu_{3\downarrow} = 0, \tag{5.56}$$

physically implying that the hopping for spin $\uparrow$ and all the local potentials are all turned off and only keep the hopping strength for spin $\downarrow$ and on-site interaction strength g. Then, the Hamiltonians become:

$$\begin{aligned} H'_{\text{vac}} &= 0 \\ H'_{\text{one-body}} &= \begin{pmatrix} 0 & 0 & 0 & 0 \\ 0 & 0 & 0 & 0 \\ 0 & 0 & 0 & -J_{23\downarrow} \\ 0 & 0 & -J_{23\downarrow} & 0 \end{pmatrix} \\ H'_{\text{two-body}} &= \begin{pmatrix} g & -J_{23\downarrow} & 0 & 0 \\ -J_{23\downarrow} & 0 & 0 & 0 \\ 0 & 0 & 0 & -J_{23\downarrow} \\ 0 & 0 & -J_{23\downarrow} & g \end{pmatrix} \end{aligned} \tag{5.57}$$

As before, the total evolution only requires a phase appearing in the two-body term, i.e. $|2\uparrow 3\downarrow\rangle$, while keeping other terms untouched. In this case, the unitary $U'_{\text{vac}} = e^{-iH'_{\text{vac}}t}$ for the vacuum-like term is still the identity due to $H'_{\text{vac}} = 0$. However, the unitary $U'_{\text{one-body}} = e^{-iH'_{\text{one-body}}t}$ for one-body terms can be obtained easily as:

$$\begin{pmatrix} 1 & 0 & 0 & 0 \\ 0 & 1 & 0 & 0 \\ 0 & 0 & \cos(-J_{23\downarrow}t) & i\sin(-J_{23\downarrow}t) \\ 0 & 0 & i\sin(-J_{23\downarrow}t) & \cos(-J_{23\downarrow}t) \end{pmatrix}. \tag{5.58}$$

Hence, we need to solve the following equation:

$$\begin{pmatrix} \cos(-J_{23\downarrow}t) & i\sin(-J_{23\downarrow}t) \\ i\sin(-J_{23\downarrow}t) & \cos(-J_{23\downarrow}t) \end{pmatrix} = \begin{pmatrix} 1 & 0 \\ 0 & 1 \end{pmatrix}. \tag{5.59}$$

The solution is easily found as $t = \frac{2n\pi}{-J_{23\downarrow}}, n \in \mathbb{Z}$ which enforces the constraint of time upon the system if we fix the hopping strength. Then, let us scrutinize the two-body unitary $U'_{\text{two-body}} = e^{-iH'_{\text{two-body}}t}$ but we are just concerned about the matrix element (2,2) of $U'_{\text{two-body}}$

because $|2\uparrow 3\downarrow\rangle$ is only two-body input in the system. We find that when $\sqrt{g^2+4J_{23\downarrow}^2}t = 2m\pi, m\in\mathbb{Z}$, this entry becomes:

$$U'(2,2) = e^{-\frac{i}{2}(g+\sqrt{U^2+4J_{23\downarrow}^2})t}. \tag{5.60}$$

Plugging in the time t obtained above, we obtain:

$$U'(2,2) = e^{-i(m+\sqrt{m^2-4n^2})\pi}, \quad m^2 \geq 4n^2 \tag{5.61}$$

This is the phase arising from the evolution in front of the term $|2\uparrow 3\downarrow\rangle$. Thus, the spin-dependent lattice can implement a phase gate. As discussed before, the CZ gate is preferable. Therefore, it would be nice to make this phase -1. One can easily observe that if $m+\sqrt{m^2-4n^2} = 2k+1$ holds, it becomes the matrix element -1. Unfortunately, this is impossible; expanding the two sides of this equation and rearranging them, one obtains:

$$4km + 2m - 4k - 1 \stackrel{?}{=} 4n^2 + 4k^2 \tag{5.62}$$

Apparently, it cannot hold since the left side is always an odd number but the right side is an even number. Thus, we need to relax the oversimplification, i.e. Eq. (5.55), by turning on more parameter in the system to see if we are capable of achieving the desired CZ gate.

Let us make the simplification to the parameters as follows:

$$-J_{23\uparrow} = -\mu_{2\uparrow} = -\mu_{3\uparrow} = -\mu_{3\downarrow} = 0 \tag{5.63}$$

where the local potential for spin $\downarrow$ at site 2 is kept. Then, the Hamiltonians become:

$$\begin{aligned}
H'_{\text{vac}} &= 0 \\
H'_{\text{one-body}} &= \begin{pmatrix} 0 & 0 & 0 & 0 \\ 0 & 0 & 0 & 0 \\ 0 & 0 & -\mu_{2\downarrow} & -J_{23\downarrow} \\ 0 & 0 & -J_{23\downarrow} & 0 \end{pmatrix} \\
H'_{\text{two-body}} &= \begin{pmatrix} -\mu_{2\downarrow}+g & -J_{23\downarrow} & 0 & 0 \\ -J_{23\downarrow} & 0 & 0 & 0 \\ 0 & 0 & -\mu_{2\downarrow} & -J_{23\downarrow} \\ 0 & 0 & -J_{23\downarrow} & g \end{pmatrix}
\end{aligned} \tag{5.64}$$

Aiming for the same goal, it is easy to find that when the following criteria are satisfied,

$$\frac{1}{2}\sqrt{\mu_{2\downarrow}^2 + 4J_{23\downarrow}^2}t = 2k\pi, k \in N \tag{5.65}$$

$$\frac{1}{2}\sqrt{(g-\mu_{2\downarrow})^2 + 4J_{23\downarrow}^2}t = l\pi, l \in N \tag{5.66}$$

the two-qubit state would be mapped to

$$e^{\frac{-i}{2}(-\mu_{2\downarrow})t}\alpha\gamma\left|1\uparrow 3\downarrow\right\rangle + \alpha\delta\left|1\uparrow 4\downarrow\right\rangle + e^{\frac{-i}{2}(g-\mu_{2\downarrow})t+il\pi}\beta\gamma\left|2\uparrow 3\downarrow\right\rangle + \beta\delta\left|2\uparrow 4\downarrow\right\rangle \tag{5.67}$$

Therefore, the relative phase here is:

$$e^{\frac{-i}{2}gt}e^{il\pi} \tag{5.68}$$

and our goal is to make it -1. The phase in first phase term is kept here because it can be removed afterwards by turning on the local potential for spin $\downarrow$ at site 3. In fact, there are many solutions to it, for example if we set parameters as:

$$l = 2,\ \ k = 1 \text{ and } \mu_{2\downarrow} = \frac{g}{2} \tag{5.69}$$

we would obtain:

$$(4J_{23\downarrow}^2 + \frac{1}{4}g^2)t^2 = 16\pi^2 \tag{5.70}$$

Moreover, the following condition must be satisfied:

$$e^{\frac{-i}{2}gt} = -1 \tag{5.71}$$

which immediately gives us

$$\frac{g}{2}t = \pm\pi \tag{5.72}$$

Then, we get

$$4J_{23\downarrow}^2 t^2 = 15\pi^2 \tag{5.73}$$

In summary, the whole procedure works as this: we first set the hopping strength $-J_{23\downarrow}$ to any value which gives a fixed time t and then the interaction strength g is obtained, giving us

the value that the local potential $-\mu_{2\downarrow}$ takes. Together, the desired CZ gate, i.e. Eq. (5.39) is achieved. Here, although local potential $-\mu_{2\downarrow}$ is unable to generate entanglement, it could alter entanglement, given that entanglement has already been formed.

We demonstrated that UQC is possible with the Hubbard model in one-dimensional spin-dependent lattice via proper control of parameters in the system. The discussion about the potential of realizing this scheme in the laboratory and the outlook of this proposal are in the next chapter.

Chapter 6

Discussion and conclusions

Through the investigation of the Hamiltonians that are within the family of the Hubbard model, a universal set of quantum gates is generated in a specially prepared one-dimensional lattice. The universality is formed by the CZ gate and single-qubit gates, which act on the logical qubits encoded in the odd-parity subspace of the Hilbert space for two qubits. Both of the spinless and spin-1/2 fermions are studied to demonstrate the possibility of performing UQC.

The physical implementation of the scheme based on interacting spinless fermions has been discussed in Sec. 5.1.2, where the main challenge is to control the n.n. interaction strength via applying external electric field to these dipolar fermionic atoms. This requires extra efforts in the laboratory so the implementation of the proposal based on the Hubbard model is our main focus in this Chapter.

The physical system proposed in Sec. 5.2 as the controlled Hubbard model to achieve UQC, features a one-dimensional double-well lattice at one-quarter filling, with spin-dependent hopping. This kind of spin-dependent double-well lattice in one dimension has already been demonstrated experimentally in the context of ultracold atomic gases [44], where polarized orthogonal optical standing waves controlled by electro-optical modulator (EOM) are overlapped to create such lattices, but the applications all have so far been focused on bosons [49, 50]. However, there are major current efforts to cool and trap two-component fermions ^{6}Li [46–48, 51] and ^{40}K [52–54] in the optical lattices to realize the Hubbard model in the laboratory.

To manipulate encoded qubits to achieve single-qubit gates and the CZ gate, one must be able to tune the hopping strength inside double wells and between adjacent double wells

and on-site potentials for fermions with different spins as discussed in Sec. 5.2.4.2. Experimentally, this has already been demonstrated to be possible [46, 48, 51, 53, 54], where a quantum gas microscope is used to image trapped fermionic atoms for manipulating tunable parameters in the system.

Additionally, it also requires the state preparation and read-out to build a quantum computer [55]. As illustrated in Fig. 5.3, our encoding requires loading spin-up and down fermions alternately in each pair of lattice sites, starting from the initialization of the $|0_L\rangle^{\otimes n}$ where all loaded fermions take up the left site of each two-site cell and the read-out of the positions of the trapped atoms also need to be performed. Both of these two requirements are successfully implemented in fermionic atoms such as ^{40}K [45, 53, 54] and ^{6}Li [46–48, 51].

Moreover, gate executions must be carried out adiabatically since the quantum information is encoded in the spatial modes rather than the internal degrees of freedom of an fermionic atom. One must avoid exciting these fermionic atoms that are in the ground state to the excited states during the sudden changes in potential when executing single-qubit and two-qubit gates. This is a main problem to be addressed. It has already been discussed in Ref. [56] but this proposal features logical qubits that are encoded in the widely-used internal states of a neural atom. Therefore, adapting the work [56] to this current scheme and applying it to specific fermionic atoms to calculate the fidelity of a gate operation are a promising subject of future work.

The non-interacting fermions (both spinless and spin-1/2) hopping between two sites in a one-dimensional lattice is mathematically linked to a special class of quantum gates called matchgates characterized by the perfect matchings in the graph theory. Expectedly, interacting spinless fermions with just n.n. interactions could break the matchgate formalism, elevating this class of quantum gates to universal quantum computation. More interestingly, spin-1/2 fermions under the Hubbard model which may be the simplest interacting model of fermionic particles also goes beyond the matchgate class to achieve universal quantum

computation. Similar works have been reported over past few years where both the Hubbard model and the Bose-Hubbard model are demonstrated to implement UQC based on quantum random walk approach [57–59].

Appendix A

The numerical results for single hopping

The table below presents arrays of data that show the numerical outcomes of the phase and amplitude of the two-body term $|2\uparrow 3\downarrow\rangle$ in Eq. (5.41) with just one hopping turned on and all one-body terms gain no phases. The evolution time is constrained by the one-body terms.

μ_2	g	Density	Phase(π)	μ_2	U	Density	Phase(π)	μ_2	g	Density	Phase(π)
0.1	-1.0	0.993012	0.00745759	0.4	-0.2	0.980642	0.0421786	0.7	0.6	0.73859	-0.163649
0.1	-0.8	0.995521	0.00598884	**0.4**	**0.0**	**1.0**	**0.0**	0.7	0.8	0.577803	-0.212813
0.1	-0.6	0.997477	0.00450487	0.4	0.2	0.980642	-0.0421786	0.8	-1.0	0.460391	0.245466
0.1	-0.4	0.998878	0.00300953	0.4	0.4	0.924252	-0.0842184	0.8	-0.8	0.614348	0.20292
0.1	-0.2	0.999719	0.00150665	0.4	0.6	0.835698	-0.125969	0.8	-0.6	0.76334	0.155565
0.1	**0.0**	**1.0**	**0.0**	0.4	0.8	0.722508	-0.167257	0.8	-0.4	0.888006	0.10518
0.1	0.2	0.999719	-0.00150665	0.4	1.0	0.59407	-0.20786	0.8	-0.2	0.970922	0.0530067
0.1	0.4	0.998878	-0.00300953	0.5	-1.0	0.465361	0.258526	**0.8**	**0.0**	**1.0**	**0.0**
0.1	0.6	0.997477	-0.00450487	0.5	-0.8	0.622976	0.209325	0.8	0.2	0.970922	-0.0530067
0.1	0.8	0.995521	-0.00598884	0.5	-0.6	0.771225	0.158276	0.8	0.4	0.888006	-0.10518
0.1	1.0	0.993012	-0.00745759	0.5	-0.4	0.892651	0.106076	0.8	0.6	0.76334	-0.155565
0.2	-1.0	0.921425	0.0494269	0.5	-0.2	0.972273	0.0531965	0.8	0.8	0.614348	-0.20292
0.2	-0.8	0.949163	0.039883	**0.5**	**0.0**	**1.0**	**0.0**	0.8	1.0	0.460391	-0.245466
0.2	-0.6	0.971164	0.0301065	0.5	0.2	0.972273	-0.0531965	0.9	-1.0	0.500339	0.240856
0.2	-0.4	0.987107	0.0201618	0.5	0.4	0.892651	-0.106076 0	.9	-0.8	0.648705	0.196998
0.2	-0.2	0.996765	0.0101078	0.5	0.6	0.771225	-0.158276	0.9	-0.6	0.787354	0.149939
0.2	**0.0**	**1.0**	**0.0**	0.5	0.8	0.622976	-0.209325	0.9	-0.4	0.900398	0.100902
0.2	0.2	0.996765	-0.0101078	0.5	1.0	0.465361	-0.258526	0.9	-0.2	0.974303	0.050716
0.2	0.4	0.987107	-0.0201618	0.6	-1.0	0.406373	0.267638	**0.9**	**0.0**	**1.0**	**0.0**
0.2	0.6	0.971164	-0.0301065	0.6	-0.8	0.572701	0.220232	0.9	0.2	0.974303	-0.050716
0.2	0.8	0.949163	-0.039883	0.6	-0.6	0.736422	0.168184	0.9	0.4	0.900398	-0.100902
0.2	1.0	0.921425	-0.0494269	0.6	-0.4	0.874832	0.113396	0.9	0.6	0.787354	-0.149939
0.3	-1.0	0.764985	0.126308	0.6	-0.2	0.967436	0.0570528	0.9	0.8	0.648705	-0.196998
0.3	-0.8	0.844452	0.101833	**0.6**	**0.0**	**1.0**	**0.0**	0.9	1.0	0.500339	-0.240856
0.3	-0.6	0.910196	0.0768075	0.6	0.2	0.967436	-0.0570528	1.0	-1.0	0.514615	0.239762
0.3	-0.4	0.959339	0.0514022	0.6	0.4	0.874832	-0.113396	1.0	-0.8	0.661186	0.195256
0.3	-0.2	0.989721	0.0257586	0.6	0.6	0.736422 -	0.168184	1.0	-0.6	0.796175	0.148144
0.3	**0.0**	**1.0**	**0.0**	0.6	0.8	0.572701	-0.220232	1.0	-0.4	0.904983	0.0994785
0.3	0.2	0.989721	-0.0257586	0.6	1.0	0.406373	-0.267638	1.0	-0.2	0.975559	0.0499368
0.3	0.4	0.959339	-0.0514022	0.7	-1.0	0.415927	0.255948	**1.0**	**0.0**	**1.0**	**0.0**
0.3	0.6	0.910196	-0.0768075	0.7	-0.8	0.577803	0.212813	1.0	0.2	0.975559	-0.0499368
0.3	0.8	0.844452	-0.101833	0.7	-0.6	0.73859	0.163649	1.0	0.4	0.904983	-0.0994785
0.3	1.0	0.764985	-0.126308	0.7	-0.4	0.8755	0.110827	1.0	0.6	0.796175	-0.148144
0.4	-1.0	0.59407	0.20786	0.7	-0.2	0.96755	0.0558974	1.0	0.8	0.661186	-0.195256
0.4	-0.8	0.722508	0.167257	**0.7**	**0.0**	**1.0**	**0.0**	1.0	1.0	0.514615	-0.239762
0.4	-0.6	0.835698	0.125969	0.7	0.2	0.96755	-0.0558974				
0.4	-0.4	0.924252	0.0842184	0.7	0.4	0.8755	-0.110827				

Table A.1: The table shows the phase and density of the two-body term $|2\uparrow 3\downarrow\rangle$. The values of parameters are bold when the unity of density is preserved.

Appendix B

The numerical results for two hoppings

Let us first take a look at simplest case where all local potentials are turned off. Since the one-body Hamiltonians are the same for spin-up and spin-down fermions, it is simplified as:

$$\begin{pmatrix} 0 & -J_{12} & 0 \\ -J_{12} & 0 & -J_{23} \\ 0 & -J_{23} & 0 \end{pmatrix} \tag{B.1}$$

Again, the goal is to map the one-body unitary based on this Hamiltonian to identity. The hopping strength $-J_{23}$ is set to -1 so all other parameters just scale with it. It is found that when $t = \frac{2\pi}{\sqrt{1+(-J_{12})^2}}$, the one-body unitary matrix becomes identity. Now, we turn to the two-body Hamiltonian which takes the following form:

$$\begin{pmatrix} 0 & -J_{12} & -J_{23} & 0 & 0 & 0 & 0 & 0 & 0 \\ -J_{12} & 0 & 0 & -J_{23} & -J_{23} & 0 & 0 & 0 & 0 \\ -J_{23} & 0 & 0 & -J_{12} & 0 & -J_{12} & 0 & 0 & 0 \\ 0 & -J_{23} & -J_{12} & g & 0 & 0 & -J_{12} & 0 & -J_{23} \\ 0 & -J_{23} & 0 & 0 & g & 0 & 0 & 0 & -J_{23} \\ 0 & 0 & -J_{12} & 0 & 0 & U & -J_{12} & 0 & 0 \\ 0 & 0 & 0 & -J_{12} & 0 & -J_{12} & 0 & -J_{23} & 0 \\ 0 & 0 & 0 & 0 & 0 & 0 & -J_{23} & 0 & -J_{12} \\ 0 & 0 & 0 & -J_{23} & -J_{23} & 0 & 0 & -J_{12} & 0 \end{pmatrix} \tag{B.2}$$

We are only concerned about the first two diagonal elements in this matrix because they are the only terms appearing in the two-body input. After running it numerically with $-J_{23} = -1$, we obtain Table B.1. It clearly demonstrates that whenever the amplitudes of the two-body terms are preserved, the interaction strength g and all their phases are zero, which fails to generate entanglement between these two qubits.

Since the previous case fails to work with all local potentials off, turning on one or more local potentials may be worth trying. Let us switch on the local potential at site 2, i.e. $-\mu_2$.

Then, the one-body Hamiltonian becomes:

$$\begin{pmatrix} 0 & -J_{12} & 0 \\ -J_{12} & -\mu_2 & -J_{23} \\ 0 & -J_{23} & 0 \end{pmatrix} \tag{B.3}$$

Again, the hopping strength $-J_{23}$ is set to -1 and after imposing the identity to the unitary matrix based on this Hamiltonian, the following conditions are found:

$$t = \frac{4n\pi}{\sqrt{4+4(J_{12})^2+\mu_2^2}}, \quad \mu_2 = \frac{2\sqrt{1+(J_{12})^2}}{\sqrt{n^2-1}} \quad or \quad t = \frac{(4m+2)\pi}{\sqrt{4+4(J_{12})^2+\mu_2^2}}, \quad \mu_2 = \frac{\sqrt{1+(J_{12})^2}}{\sqrt{m+m^2}}, \tag{B.4}$$

where t is the total evolution time and n, m are integers. Our two-body Hamiltonian takes the following form:

$$\begin{pmatrix} 0 & -J_{12} & -J_{23} & 0 & 0 & 0 & 0 & 0 & 0 \\ -J_{12} & -\mu_2 & 0 & -J_{23} & -J_{23} & 0 & 0 & 0 & 0 \\ -J_{23} & 0 & -\mu_2 & -J_{12} & 0 & -J_{12} & 0 & 0 & 0 \\ 0 & -J_{23} & -J_{12} & -2\mu_2+g & 0 & 0 & -J_{12} & 0 & -J_{23} \\ 0 & -J_{23} & 0 & 0 & g & 0 & 0 & 0 & -J_{23} \\ 0 & 0 & -J_{12} & 0 & 0 & g & -J_{12} & 0 & 0 \\ 0 & 0 & 0 & -J_{12} & 0 & -J_{12} & -\mu_2 & -J_{23} & 0 \\ 0 & 0 & 0 & 0 & 0 & 0 & -J_{23} & 0 & -J_{12} \\ 0 & 0 & 0 & -J_{23} & -J_{23} & 0 & 0 & -J_{12} & -\mu_2 \end{pmatrix} \tag{B.5}$$

Now, running it numerically with two different sets of criteria that these parameters should satisfy individually, we obtain a data table, similar to Table B.1 regardless of the values of m, n. Apparently, it shows that unless the on-site interaction g is zero, the encoded quantum information always leaks out. This again shows that local potentials cannot influence the generation of entanglement.

It seems that introducing the local potential at site 2 fails to achieve any entangling as well so let us turn to the local potential at site 3 or 1 (because they are symmetric, they should be equivalent). However, it is cumbersome to solve even the one-body unitary matrix analytically by imposing it to be identity, so the calculations are performed numerically. The data are not presented here because they give a similar pattern as was found in the previous

cases: whenever the leakage of quantum information is prevented, the corresponding on-site interaction strength g is always zero, which precludes the generation of entanglement.

J_{12}	g	Density$_1$	Density$_2$	Phase$_1(\pi)$	Phase$_2(\pi)$	J_{12}	g	Density$_1$	Density$_2$	Phase$_1(\pi)$	Phase$_2(\pi)$
0.0	-0.2	0.904628	1.0	0.0998689	0.0	0.45	-0.2	0.945212	0.929695	0.0735756	0.0773281
0.0	-0.1	0.975536	1.0	0.0499842	0.0	0.45	-0.1	0.986105	0.982005	0.0368794	0.0388727
0.0	**0.0**	**1.0**	**1.0**	**0.0**	**0.0**	**0.45**	**0.0**	**1.0**	**1.0**	**0.0**	**0.0**
0.0	0.1	0.975536	1.0	-0.0499842	0.0	0.45	0.1	0.986105	0.982005	-0.0368794	-0.0388727
0.0	0.2	0.904628	1.0	-0.0998689	0.0	0.45	0.2	0.945212	0.929695	-0.0735756	-0.0773281
0.05	-0.2	0.90532	0.994072	0.0992321	0.00247712	0.5	-0.2	0.949349	0.937642	0.0713566	0.0768499
0.05	-0.1	0.975718	0.998463	0.0496725	0.00132573	0.5	-0.1	0.98717	0.984075	0.0357531	0.0385861
0.05	**0.0**	**1.0**	**1.0**	**0.0**	**0.0**	**0.5**	**0.0**	**1.0**	**1.0**	**0.0**	**0.0**
0.05	0.1	0.975718	0.998463	-0.0496725	-0.00132573	0.5	0.1	0.98717	0.984075	-0.0357531	-0.0385861
0.05	0.2	0.90532	0.994072	-0.0992321	-0.00247712	0.5	0.2	0.949349	0.937642	-0.0713566	-0.0768499
0.1	-0.2	0.907401	0.978307	0.0973956	0.00959557	0.55	-0.2	0.952395	0.945489	0.0696258	0.0740019
0.1	-0.1	0.976265	0.994378	0.048772	0.00509620	.55	-0.1	0.987952	0.986109	0.0348754	0.0371341
0.1	**0.0**	**1.0**	**1.0**	**0.0**	**0.0**	**0.55**	**0.0**	**1.0**	**1.0**	**0.0**	**0.0**
0.1	0.1	0.976265	0.994378	-0.048772	-0.0050962	0.55	0.1	0.987952	0.986109	-0.0348754	-0.0371341
0.1	0.2	0.907401	0.978307	-0.0973956	-0.00959557	0.55	0.2	0.952395	0.945489	-0.0696258	-0.0740019
0.15	-0.2	0.910854	0.957801	0.0945658	0.0204256	0.6	-0.2	0.954463	0.952808	0.0683043	0.069587
0.15	-0.1	0.977171	0.989074	0.0473805	0.0107304	0.6	-0.1	0.988479	0.987998	0.0342075	0.0349083
0.15	**0.0**	**1.0**	**1.0**	**0.0**	**0.0**	**0.6**	**0.0**	**1.0**	**1.0**	**0.0**	**0.0**
0.15	0.1	0.977171	0.989074	-0.0473805	-0.0107304	0.6	0.1	0.988479	0.987998	-0.0342075	-0.0349083
0.15	0.2	0.910854	0.957801	-0.0945658	-0.0204256	0.6	0.2	0.954463	0.952808	-0.0683043	-0.069587
0.2	-0.2	0.915571	0.938431	0.0910429	0.0334931	0.65	-0.3	0.902432	0.911011	0.100658	0.0960533
0.2	-0.1	0.978405	0.98408	0.0456407	0.0173865	0.65	-0.2	0.955766	0.959442	0.0672933	0.0643699
0.2	**0.0**	**1.0**	**1.0**	**0.0**	**0.0**	0.65	-0.1	0.98881	0.989705	0.0336996	0.0322848
0.2	0.1	0.978405	0.98408	-0.0456407	-0.0173865	**0.65**	**0.0**	**1.0**	**1.0**	**0.0**	**0.0**
0.2	0.2	0.915571	0.938431	-0.0910429	-0.0334931	0.65	0.1	0.98881	0.989705	-0.0336996	-0.0322848
0.25	-0.2	0.921296	0.924576	0.0871656	0.0469965	0.65	0.1	0.98881	0.989705	-0.0336996	-0.0322848
0.25	-0.1	0.9799	0.980529	0.0437156	0.0241298	0.65	0.3	0.902432	0.911011	-0.100658	-0.0960533
0.25	**0.0**	**1.0**	**1.0**	**0.0**	**0.0**	0.7	-0.3	0.904205	0.923689	0.0994508	0.0880578
0.25	0.1	0.9799	0.980529	-0.0437156	-0.0241298	0.7	-0.2	0.956564	0.965326	0.0664896	0.0589908
0.25	0.2	0.921296	0.924576	-0.0871656	-0.0469965	0.7	-0.1	0.989011	0.991215	0.0332985	0.0295808
0.3	-0.2	0.927618	0.917976	0.0832573	0.0591689	**0.7**	**0.0**	**1.0**	**1.0**	**0.0**	**0.0**
0.3	-0.1	0.981547	0.978866	0.0417636	0.0301146	0.7	0.1	0.989011	0.991215	-0.0332985	-0.0295808
0.3	**0.0**	**1.0**	**1.0**	**0.0**	**0.0**	0.7	0.2	0.956564	0.965326	-0.0664896	-0.0589908
0.3	0.1	0.981547	0.978866	-0.0417636	-0.0301146	0.7	0.3	0.904205	0.923689	-0.0994508	-0.0880578
0.3	0.2	0.927618	0.917976	-0.0832573	-0.0591689	0.75	-0.3	0.905418	0.934682	0.0984014	0.0805333
0.35	-0.2	0.934031	0.917972	0.0795826	0.068655	0.75	-0.2	0.957103	0.970407	0.0657969	0.0539265
0.35	-0.1	0.983212	0.97891	0.0399175	0.0347271	0.75	-0.1	0.989145	0.992516	0.0329545	0.0270345
0.35	**0.0**	**1.0**	**1.0**	**0.0**	**0.0**	**0.75**	**0.0**	**1.0**	**1.0**	**0.0**	**0.0**
0.35	0.1	0.983212	0.97891	-0.0399175	-0.0347271	0.75	0.1	0.989145	0.992516	-0.0329545	-0.0270345
0.35	0.2	0.934031	0.917972	-0.0795826	-0.068655	0.75	0.2	0.957103	0.970407	-0.0657969	-0.0539265
0.4	-0.2	0.940029	0.922594	0.0763237	0.0747344	0.75	0.3	0.905418	0.934682	-0.0984014	-0.0805333
0.4	-0.1	0.984766	0.980143	0.038272	0.037654	0.8	-0.3	0.906517	0.943868	0.0973922	0.0739417
0.4	**0.0**	**1.0**	**1.0**	**0.0**	**0.0**	0.8	-0.2	0.957594	0.974636	0.0651325	0.0494874
0.4	0.1	0.984766	0.980143	-0.038272	-0.037654	0.8	-0.1	0.989268	0.993595	0.0326251	0.0248015
0.4	0.2	0.940029	0.922594	-0.0763237	-0.0747344	**0.8**	**0.0**	**1.0**	**1.0**	**0.0**	**0.0**

Table B.1: The table presents the phases and densities of the two-body terms when their amplitudes are within the tolerance 0.1. The Density$_1$ and the Phase$_1$ are for $|1\uparrow 3\downarrow\rangle$ and the Density$_2$ and the Phase$_2$ are for $|2\uparrow 3\downarrow\rangle$.

Bibliography

[1] R. P. Feynman. Simulating Physics with Computers. *International Journal of Theoretical Physics*, 21:467–488, June 1982.

[2] P. Shor. Polynomial-time algorithms for prime factorization and discrete logarithms on a quantum computer. *SIAM Review*, 41(2):303–332, 1999.

[3] J. I. Cirac and P. Zoller. Quantum computations with cold trapped ions. *Phys. Rev. Lett.*, 74:4091–4094, May 1995.

[4] E. Knill, R. Laflamme, and G. J. Milburn. A scheme for efficient quantum computation with linear optics. *Nature*, 409, Jan 2001.

[5] Daniel Loss and David P. DiVincenzo. Quantum computation with quantum dots. *Phys. Rev. A*, 57:120–126, Jan 1998.

[6] Alexandre Blais, Ren-Shou Huang, Andreas Wallraff, S. M. Girvin, and R. J. Schoelkopf. Cavity quantum electrodynamics for superconducting electrical circuits: An architecture for quantum computation. *Phys. Rev. A*, 69:062320, Jun 2004.

[7] T. D. Ladd, F. Jelezko, R. Laflamme, Y. Nakamura, C. Monroe, and J. L. O'Brien. Quantum computers. *Nature*, 464:45, Mar 2010. Review Article.

[8] L. Valiant. Quantum circuits that can be simulated classically in polynomial time. *SIAM Journal on Computing*, 31(4):1229–1254, 2002.

[9] D. Gottesman. The Heisenberg representation of quantum computers. *arXiv:quant-ph/9807006*, July 1998.

[10] Maris Ozols. Clifford group. *Essays at University of Waterloo, Spring*, 2008.

[11] Richard Jozsa and Akimasa Miyake. Matchgates and classical simulation of quantum circuits. *Proceedings of the Royal Society of London A: Mathematical, Physical and Engineering Sciences*, 464(2100):3089–3106, 2008.

[12] Daniel J. Brod and Ernesto F. Galvão. Extending matchgates into universal quantum computation. *Phys. Rev. A*, 84:022310, Aug 2011.

[13] Barbara M. Terhal and David P. DiVincenzo. Classical simulation of noninteracting-fermion quantum circuits. *Phys. Rev. A*, 65:032325, Mar 2002.

[14] David P. DiVincenzo and Barbara M. Terhal. Fermionic linear optics revisited. *Foundations of Physics*, 35(12):1967–1984, Dec 2005.

[15] E. Knill. Fermionic Linear Optics and Matchgates. *arXiv:quant-ph/0108033*, August 2001.

[16] C. W. J. Beenakker, D. P. DiVincenzo, C. Emary, and M. Kindermann. Charge detection enables free-electron quantum computation. *Phys. Rev. Lett.*, 93:020501, Jul 2004.

[17] L.G. Valiant. The complexity of computing the permanent. *Theoretical Computer Science*, 8(2):189 – 201, 1979.

[18] Scott Aaronson and Alex Arkhipov. The computational complexity of linear optics. In *Proceedings of the Forty-third Annual ACM Symposium on Theory of Computing*, STOC '11, pages 333–342, New York, NY, USA, 2011. ACM.

[19] David M Ceperley. An overview of quantum Monte Carlo methods. *Reviews in Mineralogy and Geochemistry*, 71(1):129–135, 2010.

[20] Matthias Troyer and Uwe-Jens Wiese. Computational complexity and fundamental limitations to fermionic quantum Monte Carlo simulations. *Phys. Rev. Lett.*, 94:170201, May 2005.

[21] Sergey B. Bravyi and Alexei Yu. Kitaev. Fermionic quantum computation. *Annals of Physics*, 298(1):210 – 226, 2002.

[22] T. E. O'Brien, P. Rożek, and A. R. Akhmerov. Majorana-based fermionic quantum computation. *Phys. Rev. Lett.*, 120:220504, Jun 2018.

[23] Stevan Nadj-Perge, Ilya K. Drozdov, Jian Li, Hua Chen, Sangjun Jeon, Jungpil Seo, Allan H. MacDonald, B. Andrei Bernevig, and Ali Yazdani. Observation of Majorana fermions in ferromagnetic atomic chains on a superconductor. *Science*, 346(6209):602–607, 2014.

[24] V. Mourik, K. Zuo, S. M. Frolov, S. R. Plissard, E. P. A. M. Bakkers, and L. P. Kouwenhoven. Signatures of Majorana fermions in hybrid superconductor-semiconductor nanowire devices. *Science*, 336(6084):1003–1007, 2012.

[25] Sankar Das Sarma, Michael Freedman, and Chetan Nayak. Majorana zero modes and topological quantum computation. *Npj Quantum Information*, 1:15001, Oct 2015. Review Article.

[26] Michael A. Nielsen and Isaac Chuang. Quantum computation and quantum information. *American Journal of Physics*, 70(5):558–559, 2002.

[27] Charles H. Bennett, Gilles Brassard, Claude Crépeau, Richard Jozsa, Asher Peres, and William K. Wootters. Teleporting an unknown quantum state via dual classical and Einstein-Podolsky-Rosen channels. *Phys. Rev. Lett.*, 70:1895–1899, Mar 1993.

[28] Christopher M Dawson. The Solovay-Kitaev algorithm. *Quantum Inf. Comput.*, 6:81, 2006.

[29] Phillip Kaye, Raymond Laflamme, and Michele Mosca. *An Introduction to Quantum Computing*. Oxford University Press, Inc., New York, NY, USA, 2007.

[30] Seth Lloyd. Almost any quantum logic gate is universal. *Phys. Rev. Lett.*, 75:346–349, Jul 1995.

[31] Deutsch David Elieser, Barenco Adriano, and Ekert Artur. Universality in quantum computation. *Proceedings of the Royal Society of London. Series A: Mathematical and Physical Sciences*, 449(1937):669–677, Jun 1995.

[32] Adriano Barenco, Charles H. Bennett, Richard Cleve, David P. DiVincenzo, Norman Margolus, Peter Shor, Tycho Sleator, John A. Smolin, and Harald Weinfurter. Elementary gates for quantum computation. *Phys. Rev. A*, 52:3457–3467, Nov 1995.

[33] Michael J. Bremner, Christopher M. Dawson, Jennifer L. Dodd, Alexei Gilchrist, Aram W. Harrow, Duncan Mortimer, Michael A. Nielsen, and Tobias J. Osborne. Practical scheme for quantum computation with any two-qubit entangling gate. *Phys. Rev. Lett.*, 89:247902, Nov 2002.

[34] Robert Raussendorf and Hans J. Briegel. A one-way quantum computer. *Phys. Rev. Lett.*, 86:5188–5191, May 2001.

[35] Michael H. Freedman, Alexei Kitaev, Michael J. Larsen, and Zhenghan Wang. Topological quantum computation. *Bull. Amer. Math. Soc. (N.S.)*, 40(1):31–38, 2003. Mathematical challenges of the 21st century (Los Angeles, CA, 2000).

[36] E. Farhi, J. Goldstone, S. Gutmann, and M. Sipser. Quantum Computation by Adiabatic Evolution. *arXiv:quant-ph/0001106*, January 2000.

[37] Leslie G Valiant. Expressiveness of matchgates. *Theoretical Computer Science*, 289(1):457–471, 2002.

[38] Henrik Bruus and Karsten Flensberg. *Many-body quantum theory in condensed matter physics - an introduction*. Oxford University Press, United States, 2004.

[39] Alexander Altland and Ben D. Simons. *Condensed Matter Field Theory*. Cambridge University Press, 2nd edition, 2010.

[40] Steven H. Simon. *The Oxford solid state basics*. Oxford University Press, Oxford, 2013. b2096210.

[41] Sergey Bravyi. Lagrangian representation for fermionic linear optics. *Quantum Info. Comput.*, 5(3):216–238, May 2005.

[42] Rudolf Grimm, Matthias Weidemller, and Yurii B. Ovchinnikov. Optical dipole traps for neutral atoms. volume 42 of *Advances In Atomic, Molecular, and Optical Physics*, pages 95 – 170. Academic Press, 2000.

[43] Tilman Esslinger. Fermi-Hubbard physics with atoms in an optical lattice. *Annual Review of Condensed Matter Physics*, 1(1):129–152, 2010.

[44] Immanuel Bloch, Jean Dalibard, and Wilhelm Zwerger. Many-body physics with ultracold gases. *Rev. Mod. Phys.*, 80:885–964, Jul 2008.

[45] G. J. A. Edge, R. Anderson, D. Jervis, D. C. McKay, R. Day, S. Trotzky, and J. H. Thywissen. Imaging and addressing of individual fermionic atoms in an optical lattice. *Phys. Rev. A*, 92:063406, Dec 2015.

[46] Anton Mazurenko, Christie S. Chiu, Geoffrey Ji, Maxwell F. Parsons, Márton Kanász-Nagy, Richard Schmidt, Fabian Grusdt, Eugene Demler, Daniel Greif, and Markus Greiner. A cold-atom Fermi-Hubbard antiferromagnet. *Nature*, 545:462, May 2017.

[47] Russell A. Hart, Pedro M. Duarte, Tsung-Lin Yang, Xinxing Liu, Thereza Paiva, Ehsan Khatami, Richard T. Scalettar, Nandini Trivedi, David A. Huse, and Randall G. Hulet. Observation of antiferromagnetic correlations in the Hubbard model with ultracold atoms. *Nature*, 519:211, Feb 2015.

[48] Maxwell F. Parsons, Anton Mazurenko, Christie S. Chiu, Geoffrey Ji, Daniel Greif, and Markus Greiner. Site-resolved measurement of the spin-correlation function in the Fermi-Hubbard model. *Science*, 353(6305):1253–1256, 2016.

[49] P. J. Lee, M. Anderlini, B. L. Brown, J. Sebby-Strabley, W. D. Phillips, and J. V. Porto. Sublattice addressing and spin-dependent motion of atoms in a double-well lattice. *Phys. Rev. Lett.*, 99:020402, Jul 2007.

[50] Bing Yang, Han-Ning Dai, Hui Sun, Andreas Reingruber, Zhen-Sheng Yuan, and Jian-Wei Pan. Spin-dependent optical superlattice. *Phys. Rev. A*, 96:011602, Jul 2017.

[51] Martin Boll, Timon A. Hilker, Guillaume Salomon, Ahmed Omran, Jacopo Nespolo, Lode Pollet, Immanuel Bloch, and Christian Gross. Spin-and density-resolved microscopy of antiferromagnetic correlations in Fermi-Hubbard chains. *Science*, 353(6305):1257–1260, 2016.

[52] Lawrence W. Cheuk, Matthew A. Nichols, Katherine R. Lawrence, Melih Okan, Hao Zhang, and Martin W. Zwierlein. Observation of 2D fermionic Mott insulators of ^{40}K with single-site resolution. *Phys. Rev. Lett.*, 116:235301, Jun 2016.

[53] Lawrence W. Cheuk, Matthew A. Nichols, Katherine R. Lawrence, Melih Okan, Hao Zhang, Ehsan Khatami, Nandini Trivedi, Thereza Paiva, Marcos Rigol, and Martin W. Zwierlein. Observation of spatial charge and spin correlations in the 2D Fermi-Hubbard model. *Science*, 353(6305):1260–1264, 2016.

[54] Matthew A. Nichols, Lawrence W. Cheuk, Melih Okan, Thomas R. Hartke, Enrique Mendez, T. Senthil, Ehsan Khatami, Hao Zhang, and Martin W. Zwierlein. Spin transport in a Mott insulator of ultracold fermions. *Science*, 2018.

[55] David P. DiVincenzo. The physical implementation of quantum computation. *Fortschritte der Physik*, 48(911):771–783.

[56] T. Calarco, E. A. Hinds, D. Jaksch, J. Schmiedmayer, J. I. Cirac, and P. Zoller. Quantum gates with neutral atoms: Controlling collisional interactions in time-dependent traps. *Phys. Rev. A*, 61:022304, Jan 2000.

[57] Andrew M. Childs, David Gosset, and Zak Webb. Universal computation by multiparticle quantum walk. *Science*, 339(6121):791–794, 2013.

[58] Ning Bao, Patrick Hayden, Grant Salton, and Nathaniel Thomas. Universal quantum computation by scattering in the Fermi-Hubbard model. *New Journal of Physics*, 17(9):093028, 2015.

[59] Michael S. Underwood and David L. Feder. Bose-Hubbard model for universal quantum-walk-based computation. *Phys. Rev. A*, 85:052314, May 2012.